~~PROPRIETARY~~

Nuclear Innovation
North America LLC
122 West Way, Suite 405
Lake Jackson, Texas 77566
979-316-3000

July 7, 2014
U7-C-NINA-NRC-140013
10 CFR 2.390

U. S. Nuclear Regulatory Commission
Attention: Document Control Desk
One White Flint North
11555 Rockville Pike
Rockville, MD 20852-2738

South Texas Project
Units 3 and 4
Docket Nos. 52-012 and 52-013
Response to Request for Additional Information

Attached are the Nuclear Innovation North America, LLC (NINA) responses to NRC staff questions in Request for Additional Information (RAI) letters 439, 440, 441, and 446 related to SRP Section 09.01.02. The attachments to this letter contain the responses to the following RAI questions:

09.01.02- 33 through 09.01.02-50 and 09.01.02-52 through 09.01.02-68

The response to RAI 09.01.02-51 will be submitted under separate cover.

Where there are COLA markups, they will be made at the first routine COLA update following NRC acceptance of the RAI responses.

This submittal contains information proprietary to Holtec International as indicated by an affidavit signed by Holtec International, the owner of the information. Attachment 37 contains the Holtec International request that this information be withheld from public disclosure pursuant to 10 CFR 2.390 and an accompanying affidavit, AFFI-2294-04, "Affidavit Pursuant to 10 CFR 2.390." This affidavit sets forth the basis on which the information in Attachments 6A and 16A may be withheld from public disclosure by the Commission and addresses with specificity the considerations listed in paragraph (b)(4) of Section 2.390 of the Commission's regulations.

Accordingly, it is respectfully requested that the information that is proprietary to Holtec International (Attachments 6A and 16A in their entirety) be withheld from public disclosure in accordance with 10 CFR 2.390 of the Commission's regulations.

D091
NRO

Correspondence with respect to the proprietary aspects of the items listed above or the supporting Holtec International Affidavit should reference AFFI-2294-04 and should be addressed to Evrim Kalfazade, Project Manager, Holtec International, Holtec Center, 555 Lincoln Drive West, Marlton, NJ 08053.

When separated from the proprietary material in Attachments 6A and 16A, this letter is not proprietary.

There are no commitments in this submittal.

If you have any questions, please contact me at (979) 316-3011 or Bill Mookhoek at (979) 316-3014.

I declare under penalty of perjury that the foregoing is true and correct.

Executed on 7/7/14

Scott Head
Manager, Regulatory Affairs
NINA STP Units 3&4

rhs

Attachments:

1. RAI 09.01.02-33
2. RAI 09.01.02-34
3. RAI 09.01.02-35
4. RAI 09.01.02-36
5. RAI 09.01.02-37
6. RAI 09.01.02-38
6A. RAI 09.01.02-38 (Prop)
7. RAI 09.01.02-39
8. RAI 09.01.02-40
9. RAI 09.01.02-41
10. RAI 09.01.02-42
11. RAI 09.01.02-43
12. RAI 09.01.02-44
13. RAI 09.01.02-45
14. RAI 09.01.02-46
15. RAI 09.01.02-47
16. RAI 09.01.02-48
16A. RAI 09.01.02-48 (Prop)
17. RAI 09.01.02-49
18. RAI 09.01.02-50
19. RAI 09.01.02-51
20. RAI 09.01.02-52
21. RAI 09.01.02-53
22. RAI 09.01.02-54
23. RAI 09.01.02-55
24. RAI 09.01.02-56
25. RAI 09.01.02-57
26. RAI 09.01.02-58
27. RAI 09.01.02-59
28. RAI 09.01.02-60
29. RAI 09.01.02-61
30. RAI 09.01.02-62
31. RAI 09.01.02-63
32. RAI 09.01.02-64
33. RAI 09.01.02-65
34. RAI 09.01.02-66
35. RAI 09.01.02-67
36. RAI 09.01.02-68
37. Affidavit

Cc: w/o attachment except*
(paper copy)

Director, Office of New Reactors
U. S. Nuclear Regulatory Commission
One White Flint North
11555 Rockville Pike
Rockville, MD 20852-2738

Regional Administrator, Region IV
U. S. Nuclear Regulatory Commission
1600 E. Lamar Blvd.
Arlington, Texas 76011-8064

Kathy C. Perkins, RN, MBA
Assistant Commissioner
Division for Regulatory Services
Texas Department of State Health Services
P. O. Box 149347
Austin, Texas 78714-9347

Robert Free
Radiation Inspections Branch Manager
Texas Department of State Health Services
P. O. Box 149347
Austin, Texas 78714-9347

*Steven P. Frantz, Esquire
A. H. Gutterman, Esquire
Morgan, Lewis & Bockius LLP
1111 Pennsylvania Ave. NW
Washington D.C. 20004

*Tom Tai
*Tarun Roy
Two White Flint North
11545 Rockville Pike
Rockville, MD 20852

(electronic copy)

*Tom Tai
*Tarun Roy
Fred Brown
U. S. Nuclear Regulatory Commission

Jamey Seeley
Nuclear Innovation North America

Peter G. Nemeth
Crain, Caton and James, P.C.

Richard Peña
Kevin Pollo
L. D. Blaylock
CPS Energy

QUESTION:

Holtec Report Section 5.3.1, "Assumptions," states, "The areas between the racks and the SFP walls are quite large, but are likely to be partially occupied by other equipment. To conservatively bound the presence of equipment in these spaces, a uniform rack-to-wall gap of 6" is modeled to provide a higher flow resistance and result in maximized computed temperatures." While the report addresses this issue for the thermal hydraulic calculations, the report does not address this for the nonlinear dynamic seismic analysis.

The staff requests the applicant to clearly describe the corresponding assumption about rack-to-wall gaps in the nonlinear dynamic seismic analysis, for consideration of potential location of equipment in the large space between the racks and the pool walls.

Provide the technical basis for concluding that the assumption in the design-basis analysis is conservative. If this is not realistic, identify the design control measures to ensure that any necessary changes to the design-basis analysis are properly implemented to account for any future changes in rack-to-wall gaps.

RESPONSE:

Based on the results of the non-linear dynamic seismic analysis, an exclusion zone has been established around the perimeter of the spent fuel racks in which no other equipment will be placed. In order to ensure that the exclusion zone is large enough to prevent any impacts with other equipment, the seismic analysis is performed in such a way as to maximize the spent fuel rack displacements. Specifically, the maximum rack-to-wall gaps (i.e., assuming no other equipment is installed in the SFP) are used as input to the non-linear dynamic seismic analysis. Since the fluid coupling force between two bodies is inversely proportional to the gap between them, the use of the maximum rack-to-wall gaps minimizes the resistance against rack seismic motion, thereby increasing the spent fuel rack displacements. The maximum lateral rack displacement from all 29 Whole Pool Multi-Rack (WPMR) analysis runs is 6.78 inches at the top of rack. At the baseplate elevation, the maximum lateral displacement is 4.72 inches. Since the rack plus the bearing pads may slide together relative to the SFP floor, the maximum lateral displacement at the base of the rack must also be imposed on the bearing pads (which extend approximately 3.81 inches beyond the edge of the rack baseplate). Therefore, the exclusion zone has been set at a distance of 11 inches from the outside face of the bumper bars (or 9.5 inches from the edge of the baseplate) on the spent fuel racks to preclude impacts with other equipment.

The response to RAI 09.01.02-66 provides a detailed description of the assumptions and results used in the additional Whole Pool Multi-Rack (WPMR) simulations that were performed to confirm that the 11-inch exclusion zone is sufficient to prevent the spent fuel racks from impacting any other equipment and ensure that the stresses in the spent fuel racks remain below allowable limits under these conditions.

Holtec Report HI-2135462 will be revised as described in the response to RAI 09.01.02-66 to establish requirements to maintain an exclusion zone around the perimeter of the spent fuel racks and the assumptions and results used in WPMR simulations that demonstrate this exclusion zone is acceptable.

QUESTION:

Holtec Report, Section 2.6, "Rack Fabrication," page 2-12, states, "The rack module manufacturing begins with fabrication of the 'box.' The boxes are fabricated from two precision formed channels by seam welding in a machine equipped with copper chill bars and pneumatic clamps to minimize distortion due to welding heat input. Figure 2.6 shows a typical box with flow holes on all four sides near the base of the box. The target minimum weld seam penetration is 80% of the box metal gauge."

In order for the staff to conclude that the boxes fabricated as stated above are acceptable, the staff requests that the applicant explain, with quantitative detail, how the acceptance criteria for the weld seams are developed to account for:

a) How is the target minimum weld seam penetration of 80% of the box metal gauge guaranteed?

b) How is the material eccentricity at the weld considered in the local stress calculation?

c) What are the significant loads (e.g., fuel assembly impact) which cause membrane and bending stresses across the weld seam?

Include a sample calculation using the worst case condition from the various analyses performed in order to demonstrate the evaluation procedure for the seam weld.

RESPONSE:

(a) & (b)

The target minimum weld seam penetration of 80% will be revised to require full penetration over the entire length of the box seam. Box seam welds will be visually inspected to ensure full thickness penetration.

Holtec Report HI-2135462, Section 2.6, Rack Fabrication, will be revised as shown by the gray shaded text below:

> The rack module manufacturing begins with fabrication of the 'box.' The boxes are fabricated from two precision formed channels by seam welding in a machine equipped with copper chill bars and pneumatic clamps to minimize distortion due to welding heat input. Figure 2.6 shows a typical box with flow holes on all four sides near the base of the box. All box seam welds are visually inspected to ensure full thickness penetration.

(c) The most significant load that drives the seismic response of the racks and causes membrane and bending stresses in the cell assemblage is the fuel-to-cell impact load. The response to RAI 09.01.02-49 describes the method used to evaluate the capability of a single cell wall to withstand the maximum fuel-to-cell impact load. A sample calculation for the seam weld is not provided for the reason given in the response to (a) & (b) above.

QUESTION:

FIGURE 1.1.1 – LAYOUT FOR STP 3 & 4 ABWR FUEL STORAGE RACKS, on page 1-3 of the Holtec Report, provides gaps between adjacent racks to be 5 ¼" (+/-1/4").

The applicant is requested to clearly indicate in the figure the elevation of the rack-to-rack gaps. Confirm that these are the gaps between the bumper bars at the top of the racks.

RESPONSE:

The rack-to-rack gaps are measured from the outside faces of the rack cells at the top of the rack and do not include the thickness of the bumper bars (0.5" thick). Therefore, the bumper bar-to-bumper bar gaps are 4 ¼" (+/-1/4"). The design drawing includes a note to clearly state the elevation of the shown gaps.

Holtec Report HI-2135462, Figure 1.1.1, layout for STP 3 & 4 ABWR Fuel Storage Racks, will be revised to add a similar note as shown by the gray shaded text below:

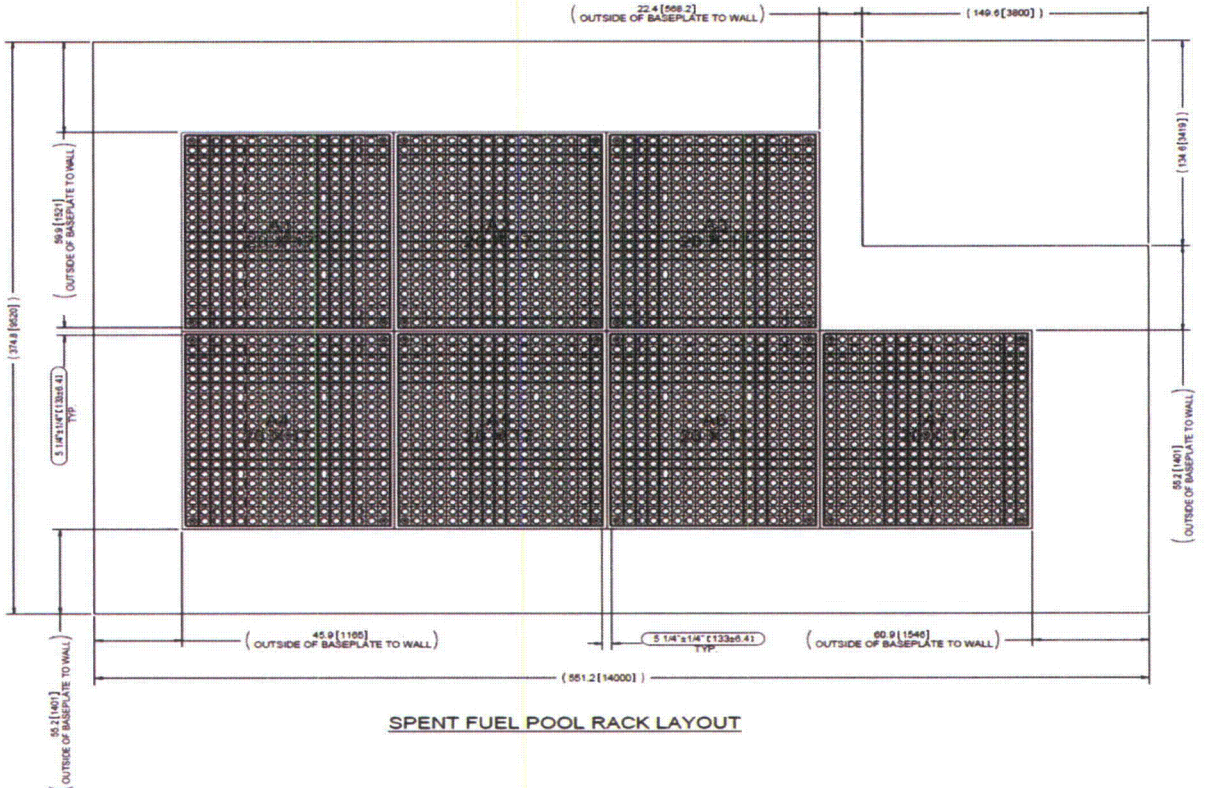

FIGURE 1.1.1 – LAYOUT FOR STP 3 & 4 ABWR FUEL STORAGE RACKS (For Reference Only)

Notes:

1. All dimensions are approximate and provided in inches and [millimeters].
2. The rack-to-rack gaps are measured from the outside faces of the rack cells at the top of the rack and do not include the thickness of the bumper bars (0.5" thick).

QUESTION:

Holtec Report Section 2.1, "Introduction," states, "The overall design of the SFP storage rack modules is similar to those presently in service in the spent fuel pools at numerous other nuclear plants. Holtec has provided thousands of storage cells of this design to various nuclear plants around the world."

Given the considerable amount of normal operating experience around the world, the staff requests the applicant to describe:

(1) If there is any operating experience related to any adverse impact on structural integrity of the racks, and

(2) How the STP fuel rack design addresses such previously observed problems. Discuss whether there is any potential for interaction between stainless steel and Metamic that would degrade the stainless steel rack materials, and if so, how the degraded condition is considered in the design.

RESPONSE:

(1) Since the spent fuel racks are fabricated using stainless steel and their design does not include any active systems, they are not susceptible to long-term structural degradation. The only situation where operating experience has shown the potential for an adverse impact on structural integrity of the spent fuel racks is when a rack is installed directly beneath a vertically oriented discharge pipe for the Spent Fuel Pool (SFP) cooling system. Depending on the proximity of the pipe to the top of the spent fuel rack and the flow rate of the SFP cooling water, the direct impingement of the cooling water on the spent fuel rack can cause flow induced vibration of the cell walls, which over time can lead to localized weld failures due to fatigue. This is not a concern for the STP 3&4 spent fuel racks because the discharge diffuser pipe for the SFP cooling system is located at the bottom of the pool. .

(2) Holtec's operating experience using Metamic, as well as in-service coupon testing at several nuclear sites, has shown no evidence of any adverse interaction between stainless steel and Metamic. In addition, Holtec and EPRI have performed extensive testing of Metamic coupons under various conditions (e.g., at elevated temperature, under irradiation, in boric acid solution, etc.), and the results indicate that Metamic is exceptionally stable in the typical SFP environment. These test results[1] have been submitted to the NRC, and the staff has previously approved the use of Metamic for spent fuel rack applications[2].

---

[1] "Sourcebook for Metamic Performance Assessment", by Dr. Stanley Turner, Holtec Report HI-2043215, Rev. 2, Docket No. 71-9261 (TAC L24029). (Holtec Proprietary)

[2] "Safety Evaluation by the Office of Nuclear Reactor Regulation Related to Holtec International Report HI-2022871 Regarding Use of Metamic in Fuel Pool Applications," Facility Operating License Nos. DPR-51 and NPF-6, Entergy Operations, Inc., docket No. 50-313 and 50-368, USNRC, June 2003.

QUESTION:

Holtec Report Section 2.6, "Rack Fabrication," describes the design of the spent fuel racks in the context of the fabrication methodology. Several statements in Section 2.6 require clarification and/or further explanation, in order for the staff to completely understand the rack design, including the welding of the various components to produce the finished rack.

(a) The third paragraph states, "Each box constitutes a storage location, as shown in Figure 2.2. Furthermore, when the boxes are secured together via tie bars (shown in Figures 2.10 and 2.11) into racks, there are also storage locations between the boxes." The staff notes that Figure 2.3 identifies "filler panels" that are required to complete the cells on the periphery of the rack. However, there is no description of the filler panel design and method of joining to the otherwise completed rack. Provide design and fabrication details for the filler panels, comparable to the information provided for the rest of the rack.

(b) The fourth paragraph states, "The baseplate is attached to the box assemblage by fillet welding the perimeter of the box assemblage to the baseplate as shown in Figure 2.9." Figure 2.9 includes the note. "WHERE POSSIBLE ON ALL RACKS". Based on past fabrication of similar racks, show a plan view of the actual fillet weld path around the perimeter of the box assemblage. What weld geometry assumption is used in the calculation of stress in the fillet weld?

(c) The sixth (last) paragraph states, "Appropriate NDE (nondestructive examination) occurs on all welds including visual examination of sheathing welds, box longitudinal seam welds, box assemblage-to-baseplate welds, and tie bar welds, as well as liquid penetrant examination of support leg welds." The staff interpreted this to mean that all the welds, including the support leg welds, receive visual examination, but only the support leg welds receive liquid penetrant inspection. Please confirm the staff's interpretation or clarify the NDE program. Also explain why liquid penetrant examination is applied to, and only to, the support leg welds.

RESPONSE:

(a) Holtec Report HI-2135462, Section 2.6, Rack Fabrication, will be revised to include a description of the filler panel design and method of joining as shown in the response to RAI 09.01.02-39.

(b) Holtec Report HI-2135462, Figure 2.9, will be revised to change the weld note from "WHERE POSSIBLE ON ALL RACKS" to "EXCEPT AT FLOW HOLE LOCATIONS." A copy of the revised Figure 2.9 is shown below.

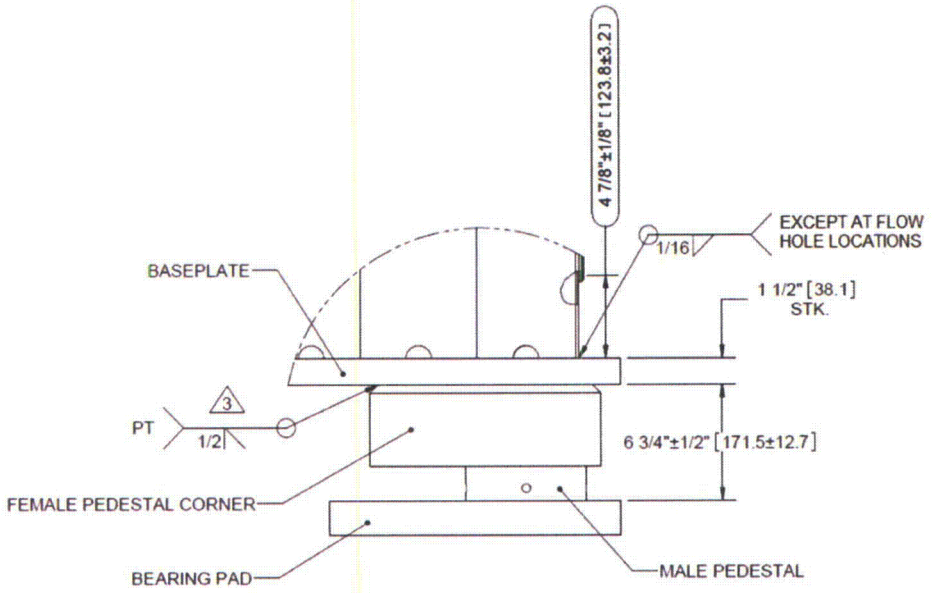

(TYPICAL FOR ALL RACKS)

FIGURE 2.9: ELEVATION VIEW DETAIL F

(c) The staff's interpretation of the NDE program is correct. The liquid penetrant examination is applied to the support leg welds for defense in depth since the support leg is the most heavily loaded component in the spent fuel rack. This exceeds the requirements of the ASME Code as explained below.

Per Appendix D to SRP 3.8.4 (Rev. 3), the design, fabrication, and installation of spent fuel racks of stainless steel material may be performed based on ASME Code, Section III, Division 1, Subsection NF requirements for Class 3 component supports. Accordingly, the examination of Class 3 support welds is governed by NF-5231, which states:

(a) Primary member welded joints that have a groove depth or throat dimension greater than 1 in. (25 mm) shall be examined by the liquid penetrant or magnetic particle method, except that the exposed ends of welds need only be visually examined.

(b) Primary welded joints exclusive of those described in NF-5231(a) shall be examined by visual method. Since all of the welded joints on the spent fuel racks are smaller than 1 inch, only visual examination is required.

09.01.02-38

Holtec Report "CHAPTER 7: MECHANICAL ACCIDENT EVALUATION" describes the evaluation conducted for the accidental drop of a fuel assembly over the top of a spent fuel storage rack. The staff requests the applicant to clarify several aspects of the evaluation, to assist the staff in making its determination of acceptability.

Section 7.1.2.1, "Calculation of Incident Impact Velocity," identifies the equations used to calculate the impact velocities for the 3 postulated drop scenarios. The staff is not clear how these equations were actually applied in the calculation.

(1) Is the first equation used for the shallow drop case to get the velocity at the top of the rack, and then the second equation used to get the velocity increase from the top of the rack down to the baseplate, for the deep drop scenarios?

(2) What is the technical reference for and the value of "C_D" used in the first equation?

(3) Is the function "f" in the second equation derived from testing or theory? Cite the reference. How sensitive is the value of "f" to small changes in the parameters that are identified (x, v, d_1, d_2, A_1, A_2)?

RESPONSE:

(1) Yes, the first equation is used for the shallow drop case to determine the velocity at the top of the rack, and the second equation is used for the deep drop scenarios to determine the velocity increase from the top of the rack to the baseplate.

The methodology used to calculate the impact velocity of the dropped fuel assembly is the same methodology used in the AP1000 spent fuel rack application.

(2) The drag coefficient (C_D) used in the analysis is equal to 0.99. This value, which is applicable to a long slender cylinder having a trajectory parallel to its longitudinal axis, is obtained from Table 11.4.4 of Marks' Standard Handbook for Mechanical Engineers (10^{th} Edition). In reality the fuel assembly is not a solid bar; the lower nozzle block of the fuel assembly may have small flow holes, which allow water to pass between the fuel rods. Although these flow holes reduce the form drag of the lower nozzle, they introduce significant energy loss at the entrance of each flow hole and significant internal flow resistance at the grid spacers and on the fuel rod surfaces. Thus, a solid cylinder is considered to reasonably represent the real behavior of the fuel assembly. However, to ensure a conservative estimate of the fuel assembly's impact velocity, the frontal area of fuel assembly is taken as roughly 40% of the enveloping area of the fuel assembly cross section.

(3) The function "f", which represents the total fluid resistive force due to form drag and the confinement of fluid flow in a storage cell, is derived from fluid mechanics principles, as shown in in the following pages of this RAI response (Attachment 6A) which is excerpted from Holtec calculation package HI-2135571.

QUESTION

Holtec Report "CHAPTER 6: STRUCTURAL/SEISMIC EVALUATION" describes the analysis methodology, STP racks modeling, and the seismic analysis results. The staff requests the applicant to clarify several aspects of the evaluation, to assist the staff in making its determination of acceptability.

(a) Section 6.2.1, "Fuel Acceptance Criteria," states, "It is noted that the spent fuel assemblies are not expected to suffer any damage while stored inside the spent fuel storage racks. This is because the lateral impact loads that occur inside a spent fuel storage rack are much smaller than the impact loads associated with transportation packages certified under 10 CFR 71. For example, the HI- STAR 100 transportation package is qualified for a 9-meter drop accident resulting in a 60g impact load [6.2.2]." Is the transportation package loaded with embrittled spent fuel? What is the 9-meter drop orientation – transportation package vertical or transportation package horizontal? Is support of the fuel inside the transportation package comparable to the support conditions in a spent fuel rack cell?

(b) Section 6.2.2, "Rack Acceptance Criteria," states, "The worst thermal stress field in a fuel rack is obtained when an isolated storage location has a fuel assembly generating heat at maximum postulated rate and surrounding storage locations contain no fuel. Heated water makes unobstructed contact with the inside of the storage walls, thereby producing maximum possible temperature difference between adjacent cells."

Section 6.7.3.2, "Analysis of Thermal Effects," states, "A conservative estimate of weld stresses along the length of an isolated hot cell can be obtained by considering a beam strip uniformly heated by 50°F, which is restrained from growth along one long edge. The above thermal gradient is based on the results of the thermal-hydraulic analysis, which show that the difference between the local cell maximum temperature (184°F per Table 5.5.1 in chapter 5 of this report) and the corresponding bulk pool temperature (150.8°F) is less than this value;" and "Using shear beam theory and subjecting the strip to a uniform temperature rise AT = 50°F, one can calculate an estimate of the maximum value of the average shear stress in the strip."In order for the staff to determine the adequacy of the thermal analysis performed by the applicant, the staff requests the applicant to provide the following:

(1) Clarify whether the calculation in Chapter 5 is based on the same assumption (i.e., an isolated storage location has a fuel assembly generating heat at the maximum postulated rate and surrounding storage locations contain no fuel). From the bulk pool temperature, it would appear that this is not the case. Correct the text of the report as necessary, to clearly describe the basis for the 50°F temperature differential used in the calculation.

(2) Provide a figure in the report that clearly shows the simplified beam model used for the thermal stress calculation, including coordinate system, boundary conditions, dimensions and loading.

(3) Explain the origin of the denominator "0.931" in the equation for maximum shear stress shown on page 6-26 of the report.

(c) Section 6.7.9, "Weld Stresses," Paragraph a, "Baseplate-to-Rack Cell Welds," shows a picture of fillet welds on 4 sides of the cell attaching to the baseplate. From the description of the fabrication sequence in Section 2.6, "Rack Fabrication," 4th paragraph, the staff understood that only the perimeter of the assembled rack is fillet-welded to the baseplate. The text states, "The baseplate is attached to the box assemblage by fillet welding the perimeter of the box assemblage to the baseplate as shown in Figure 2.9." Clarify that all 4 sides of every cell are fillet-welded to the baseplate, consistent with the picture shown in Section 6.7.9. Correct the text in the 4th paragraph of Section 2.6 and add a figure that clearly indicates this. Describe the fabrication sequence that accomplishes this. The current description appears to indicate that all cells forming a rack are joined together prior to welding to the baseplate.

(d) Section 6.7.10, "Potential for Cell Wall Buckling," presents a summary of a hand calculation using a classical buckling formula, with K = 3.44. There is no technical basis provided for using this value of K. Add a figure to the report depicting the simplified buckling model, showing the coordinate system, dimensions, boundary conditions, and loading. Provide the technical basis for the conservatism of the simplified model, the assumed boundary conditions, and the selected value of K.

(e) Table 6.6.2, "Maximum Values of Lateral Displacements," presents extremely limited displacement data. To assist the staff in its technical review, expand this table to include the top-of-rack and baseplate maximum displacements for each of the 21 cases analyzed.

RESPONSE:

(a) The HI-STAR 100 cask is licensed to transport fuel with burnup less than 45,000 MWD/MTU. The effects of fuel embrittlement are not considered in the HI-STAR 100 SAR (More recent submittals, such as the HI-STAR 180 transport cask, are licensed for high burnup fuel and include detailed structural and criticality analyses considering the effects of fuel embrittlement). In accordance with 10 CFR 71.73, the HI-STAR 100 transport package has been analyzed for a wide range of drop orientations, including top and bottom end drops, horizontal side drop, center-of-gravity over corner drop, and shallow angle drops (i.e., slap down), which are documented in the HI-STAR 100 SAR (Docket No. 71-9261). Also, the support of the fuel assemblies inside the transport package is comparable to the support conditions in a spent fuel rack cell. The figure below shows a typical 32 assembly fuel basket, which is used to support the fuel assemblies inside the HI-STAR 100 transport cask. Similar to a spent fuel rack, the fuel assemblies are stored inside a continuous cell box that supports the fuel assembly over its full length. Additional information about the capability of irradiated fuel to withstand impact loads is presented in the response to RAI 09.01.02-45.

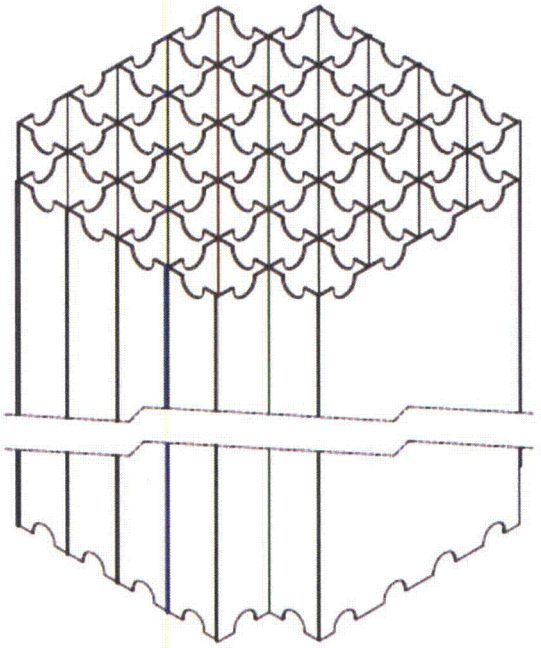

Typical Fuel Basket Used to Store Fuel Inside HI-STAR 100 Cask

(b) (1) The thermal calculations described in Chapter 5 do not include a scenario with a maximum heat fuel assembly surrounded by empty cells, as such a scenario would not yield the maximum local temperature. The maximum local water temperature is computed based on the maximum bulk water temperature assuming that all spent fuel rack storage locations are occupied. The difference between the local and bulk water temperatures provides a reasonable estimate for the temperature gradient between an empty cell location and a loaded cell. This is because the local water temperature increases/decreases commensurately with the bulk water temperature as the total heat load in the SFP rises/falls. Per Table 5.5.1 of Holtec Report No. HI-2135462, the maximum calculated local water temperature is 185°F. The corresponding bulk water temperature for the same heat load conditions is 150.8°F. Thus, the difference between the local and bulk water temperatures is 34.2°F. For conservatism, a bounding temperature gradient of 50°F is used to evaluate the thermal stresses associated with an isolated hot cell.

Accordingly, the text in Section 6.7.3.2, Analysis of Thermal Effects, of Holtec Report No. HI-2135462 will be revised as shown by the gray shaded text below:

The most severe thermal gradient between cells will develop when an isolated storage location contains a fuel assembly emitting maximum postulated heat, while the surrounding locations are empty. A conservative estimate of weld stresses along the length of an isolated hot cell can be obtained by considering a cell uniformly heated by 50°F, which is restrained from growth by the intermittent cell-to-cell welds along its corner edges. The above thermal gradient is based on the results of the thermal-hydraulic analysis, which show that the difference between the local cell maximum temperature

(185°F per Table 5.5.1 in chapter 5 of this report) and the corresponding bulk pool temperature (150.8°F) is only 34.2°F. The difference between the local and bulk water temperatures provides a reasonable estimate for the temperature gradient between an empty cell location and a loaded cell. This is because the local water temperature increases/decreases commensurately with the bulk water temperature as the total heat load in the SFP rises/falls. To insure that the results of the analysis are conservative, a bounding temperature gradient of 50°F is used as input.

The Combined License Application (COLA), Part 2, Tier 2, Subsections 9.1.2.1.4, Thermal-Hydraulic Design, and 9.1.6.8, Spent Fuel Racks Thermal-Hydraulic Analysis, describe the requirement for a thermal-hydraulic analysis of the spent fuel racks to demonstrate sufficient natural convection coolant flow to remove decay heat without reaching excessive water temperatures which will be verified for the as-built spent fuel racks by ITAAC 2.5.6.4. Holtec International Licensing Report HI-2135462, Chapter 5, Thermal-Hydraulic Evaluation, provides the thermal-hydraulic analyses for the spent fuel rack required by Part 2, Tier 2, Subsections 9.1.2.1.4 and 9.1.6.8. Therefore, Part 2, Tier 2, Subsections 9.1.2.1.4 and 9.1.6.8, will be revised as shown in the gray shaded text below:

9.1.2.1.4 Thermal-Hydraulic Design

The fuel storage racks are designed to provide sufficient natural convection coolant flow to remove decay heat without reaching excessive water temperatures (100°C). In the spent-fuel storage pool, the bundle decay heat is removed by recirculation flow to the fuel pool cooling heat exchanger to maintain the pool temperature. Although the design pool exit temperature to the fuel pool cooling heat exchanger is far below boiling, the coolant temperature within the rack is higher, depending on the naturally induced bundle flow which carries away the decay heat generated by the spent fuel. The purchase specification for the fuel storage racks require the vendor to perform the thermal-hydraulic analyses to evaluate the rate of naturally circulated flow and the maximum rack water exit temperature. Holtec International Licensing Report HI-2135462, Chapter 5, Thermal-Hydraulic Evaluation, provides the required analyses. See Subsection 9.1.6.8 for COL license information requirements.

9.1.6.8 Spent Fuel Racks Thermal-Hydraulic Analysis

The following standard supplement addresses COL License Information Item 9.8.

The COL applicant shall provide the NRC confirmatory thermal-hydraulic analysis that evaluates the rate of naturally circulated flow and the maximum rack water exit temperatures, as required by Subsection 9.1.2.1.4. Holtec International Licensing Report HI-2135462, Chapter 5, Thermal-Hydraulic Evaluation, provides the required analyses. ~~A confirmatory thermal-hydraulic analysis will be prepared and verified in accordance with ITAAC 2.5.6.4.~~

Fuel bundle data in the analysis ~~will~~ used maximum decay heat generation rates for worst case power history. Natural circulation flow through the rack arrangement prevents water temperatures from exceeding 100°C under normal, abnormal, and accident conditions.

(b) (2)&(3)

The beam strip model previously used to calculate the shear stress in the cell-to-cell weld due to thermal effects has been deleted from Section 6.7.3.2 of Holtec Report HI-2135462 and replaced by the following:

The shear stress in the cell-to-cell welds due to the effects of an isolated hot cell is determined by assuming that the cell-to-cell welds fully restrain the cell's thermal growth. Thus, the restraint force, F, acting on a group of four cell-to-cell welds (one at each corner of the cell) is calculated using the following equation:

$$F = E\alpha\Delta T A_{cell}$$

where E is the Young's modulus of the cell material (= 27.5 × 106 psi), α is the coefficient of thermal expansion of the cell material (= 9.4 × 10-6 in/in/°F), ΔT is the temperature rise (= 50°F), and Acell is the cross-sectional area of a single cell (= 2.29 in2). The resulting value for F is 29,620 lbf.

The shear stress, τ, in each cell-to-cell weld is then calculated as:

$$\tau = \frac{F}{4A_{weld}}$$

where Aweld is the effective throat area of a single cell-to-cell weld (= 0.318 in2). The resulting value for τ is 23,270 psi.

Strictly speaking thermal stresses do not require evaluation under Subsection NF per NF-3121.11 [6.2.5]. However, for conservatism, the above calculated stress is compared against the primary plus secondary stress limit per Table NF-3523(b)-1 of the ASME Code [6.2.5]. Specifically, the stress limit is the lesser of 2Sy or Su at the applicable temperature. For SA-240 304L material, the limit is controlled by 2Sy, which equals 42,800 psi based on the material yield strength given in Table 6.5.1. Therefore, there is a safety
factor = 42,800 / 23,270 = 1.84 against cell wall shear failure due to secondary thermal stresses from cell wall growth under the worst case hot cell condition.

(c) Each cell box is welded to the baseplate on all four sides, including the perimeter of the box assemblage. During fabrication, the baseplate is positioned in a fixture and the cell boxes are individually welded to the baseplate one at a time from the center outward until the entire rack is assembled.

Holtec Report HI-2135462, Section 2.6, Rack Fabrication, will be revised to provide additional description as shown in the gray shaded text below:

The composite box assemblies are joined together in a fixture using tie bars. Figure 2.1 shows an elevation view of storage cells of a typical BWR rack module. Joining the cells by the tie bars results in a well-defined shear flow path and essentially makes the box assemblage into a multi-flanged beam-type structure. As shown in Figure 2.3, filler panels, as well as the corner angles, are used to cap off the developed cells around the perimeter of the rack. The filler panels and corner angles are fabricated from the same thickness material as the cell boxes. The width of the filler panels is slightly larger than the inner dimension of the storage cell such that when a filler panel is positioned in place it overlaps the exterior walls of the adjacent cell boxes. A corner angle, which is wider than a filler panel and has a 90 degree bend, is used where a developed cell is situated at an outside corner of the rack cell assemblage (see Figure 2.3). The vertical edges of the filler panels and corner angles are welded directly to its neighboring cell boxes through a series of intermittent fillet welds without any tie bars. The length and spacing of the intermittent fillet welds that join the filler panels and corner angles match the locations of the tie bar welds between cell boxes. Each filler panel is equipped with a stainless steel sheathing, which holds a single Metamic panel, in the same manner as the cell boxes. Each corner angle has two Metamic panels affixed to its two outside faces.

The "baseplate" is attached to the bottom of the box assemblage. During formation of the rack in the fixture, each composite box assembly is also individually welded to the rack "baseplate" along all four sides. The baseplate is an austenitic stainless steel plate that has large diameter holes (except at lift locations that have irregular shaped cut-outs of similar area) cut out in a pitch identical to the box pitch. In addition to the interior box-to-baseplate welds, the perimeter of the box assemblage is welded to the baseplate as shown in Figure 2.9. Bumper bars are stainless steel plates that are welded along the perimeter of the rack to prevent mislocation of a fuel assembly between racks and to minimize the impact loads generated during a seismic event.

(d) Holtec Report HI-2135462, Section 6.7.10, Potential for Cell Wall buckling, will be replaced with a more detailed finite element analysis of the cell wall bucking that is provided in the response to RAI 09.01.02-64.

(e) Holtec Report HI-2135462, Table 6.6.2, Rack Displacements, will be revised as shown in the response to RAI 09.01.02-66 to include the maximum rack displacement relative to floor at both the top of the rack and the baseplate for all of all of the Whole Pool Multi-Rack (WPMR) analysis runs discussed in HI-2135462.

(e) (1) Consistent with part (b) (1) of this response, Holtec International Licensing Report HI-2135462 is incorporated by reference into the STP 3 & 4 COLA as supplemental information to the ABWR DCD (i.e., incorporated by reference into the STP 3 & 4 FSAR). Incorporation by reference of HI-2135462 into the FSAR is a supplement to Section 1.6 and Table 1.1.6-2 of the ABWR DCD. Therefore, Part 2, Tier 2, Subsection 1.6 and Table 1.6-2, will be revised as shown in the gray shaded text below:

1.6 GE Topical Reports and Other Documents

STD DEP Admin

The information in this section of the reference ABWR DCD, including all tables, is incorporated by reference with the following supplement.

Table 1.6-2 is a supplemental tabulation of ~~GE Topical~~ Reports incorporated by reference as part of the combined license application.

Table 1.6-2 Additional ~~Topical~~ Reports Incorporated by Reference

Report No.	Title	Referenced in FSAR Section
NEDO-32686-A	Utility Resolution Guidance for ECCS Suction Strainer Blockage, October 1998	App 6C
HI-2135462	Holtec International Licensing Report for South Texas Project Units 3 & 4 ABWR Spent Fuel Racks	9.1

(e) (2) The ABWR DCD provides new fuel storage racks in the New Fuel Vault but was written to recognize that new fuel must be placed in the racks in the spent fuel pool before being loaded into the reactor. Standard Departure T1 2.5-1, Elimination of New Fuel Storage Racks From the New Fuel Vault, eliminates the new fuel storage racks because new fuel can be safely stored in the fuel racks in the spent fuel pool. FSAR Section 3.1.2.6.3.2, Evaluation Against Criterion 62, will be revised as shown by the gray shaded text below to clarify that there are no designated new fuel racks:

3.1.2.6.3.2 Evaluation Against Criterion 62

STP DEP T1 2.5-1

Appropriate plant fuel handling and storage facilities are provided to preclude accidental criticality for new and spent fuel. Criticality in new and spent fuel storage is prevented by presence of fixed neutron absorbing material. Fuel elements are limited by rack design to only top-loaded fuel assembly positions. The ~~new and spent~~ fuel racks are Seismic Category I components.

~~New fuel is placed in dry storage in the top-loaded new fuel storage vault. This vault contains a drain to prevent the accumulation of water. Neutron absorbing material in the new fuel storage vault racks prevents an accidental critical array, even in the event the vault becomes flooded or subjected to seismic loadings.~~

(e) (3) ABWR DCD 9.1.6.2, Dynamic and Impact Analyses of New Fuel Storage Racks, requires that the COL applicant provide confirmatory dynamic and impact analyses of the new fuel storage racks, as specified in Subsection 9.1.1.1.6. COLA Part 2, Tier 2, Section 9.1.6.2, identifies this requirement as COL License Information Item 9.2.

Standard Departure T1 2.5-1 eliminates the new fuel storage racks because new fuel can be safely stored in the fuel racks in the spent fuel pool as discussed in (e) (2) above. Therefore, COL License Information Item 9.2 requirements for the dynamic and impact analyses for the racks where new fuel is stored are satisfied by the dynamic and impact analyses of the spent fuel racks.

To clarify that COL License Information Item 9.2 requirements for dynamic and impact analyses for the racks that hold new fuel is met by the dynamic and impact analyses of the fuel storage racks in the spent fuel pool, COLA Part 2, Tier 2, Section 9.1.6.2, will be revised as shown by the gray shaded text below:

9.1.6.2 Dynamic and Impact Analyses of New Fuel Storage Racks

The following standard supplement addresses COL License Information Item 9.2.

The COL applicant shall provide the NRC confirmatory dynamic and impact analyses of the new fuel storage racks, as requested by Subsection 9.1.1.1.6.

The new fuel storage racks in the new fuel vault were eliminated by STP DEP T1 2.5-1. New fuel will be stored in the fuel storage pool.

See Subsections 9.1.6.4 and 9.1.6.7.

QUESTION:

In section 6.2.3.1.2, "Level D Service Limit," of HOLTEC Report, HI2135462, the applicant calculated a factor of 1.8, which is the quotient of (Level D shear stress limit of material yield strength) / (Level A shear stress limit of material yield strength) = 0.72Sy / 0.4Sy. However, a factor from the quotient of (Level D shear stress limit of material ultimate strength) / (Level A shear stress limit of material ultimate strength) = 0.42Su / 0.3Su would be 1.4. The staff requests that the applicant provide a discussion assuring that a factor of 1.8 is a conservative to determine the weld allowable stress limit for Service Level D.

RESPONSE:

Per NF-3322.1(b)(2), the Level A shear stress limit of 0.3Su only applies to beam end connections where the top flange is coped or in situations where failure might occur by shear along a plane through the fasteners. Neither of these situations is applicable to the STP 3 & 4 spent fuel racks. The Level A shear stress limit that governs the spent fuel rack design is 0.4Sy per NF-3322.1(b)(1). For Level D conditions, the governing shear stress limit is 0.72Sy based on the construction material (SA-240 304) for the spent fuel racks (i.e., 0.72Sy is less than 0.42Su). Therefore, the Level D to Level A shear stress ratio is 0.72Sy / 0.4Sy = 1.8. This ratio has been used consistently by Holtec to compute the Level D weld stress limit for numerous spent fuel rack applications, which have been approved by the NRC.

The increase factor of 1.8 is calculated because the 1989 Edition of the ASME Code Section III, which is the design code for the STP 3 & 4 spent fuel racks, does not give a weld allowable stress limit for Service Level D. It is noted that beginning with the 2010 Edition of the ASME Code, the weld allowable stress limit for Service Level D is specified as 0.51Su (or 1.7 times the weld allowable stress limit for Service Level D). Although the 2010 Edition of the ASME Code Section III does not apply to STP 3 & 4 spent fuel racks, the calculated weld stresses presented in Chapter 6 of Report No. HI-2135462 are all below 0.51Su.

QUESTION:

Holtec Report Section 2.3 lists the applicable codes and standards. Explain why different versions of ASME codes are used, i.e., 1989 and 2007 editions for Section III and 2010 Edition for Section II.

RESPONSE:

Holtec Report HI-2135462, Section 2.3, Applicable Codes and Standards, Part a, Design Codes, includes the following references:

(4) ASME B&PV Code Section III, Subsection NF-3000 and NF-5000, 1989 Edition, which establishes requirements related to the design, fabrication, and examination of supports;

(5) ASME B&PV Code Section III, Subsection NCA-3862, 2007 Edition, which establishes requirements related to certification of material;

(6) American Society for Nondestructive Testing SNT-TC-1A, "Recommended Practice for Personnel Qualifications and Certification in Nondestructive Testing", 2011 Edition, which establishes requirements for nondestructive testing; and,

(7) ASME B&PV Code, Section II, 2010 Edition, which establishes requirements related to material and material properties.

For reference (4), the use of the 1989 edition of ASME B&PV Code Section III, Subsection NF-3000 and NF-5000, for design, fabrication, and examination of supports for spent fuel racks is consistent with both ABWR DCD and FSAR, Table 1.8-21, Industrial Codes and Standards Applicable to ABWR.

For reference (5), the 2007 Edition of the ASME B&PV Code Section III, Subsection NCA-3862, 2007 Edition, for "certification of material" is not used in HI-2135462 and has no material effect on the analysis or analysis results. ABWR DCD 9.1.2 requires that that the spent fuel racks are fabricated from materials "specified in accordance with the latest issue of applicable ASTM specifications at the time of equipment order" which facilitates material procurement. Therefore, HI-2135462, Section 2.3, Reference (5) will be deleted.

For reference (6), the 2011 edition of ASNT SNT-TC-1A standard was inadvertently referenced in the licensing report but is not needed because ASME B&PV Code, Section III, Subsection NF-5000 (1989) already cites SNT-TC-1A (1984 Edition). Therefore, HI-2135462, Section 2.3, Reference (6) will be deleted. Note that suppliers generally conform to the latest codes and standards in effect at the time of purchase. Consequently, at the time of procurement and fabrication, the codes and standards used, if later than those specified, will be reconciled to ensure that the codes and standards in effect meet or exceed those specified in the licensing requirements.

For reference (7), HI-2135462, Section 6.2.3.1, Limits from the ASME Code, does reference the 2010 edition of ASME B&PV Code Section II, in that material properties listed in Table 6.5.1 are from ASME Code Section II, Part D. The Specification for Heat-Resisting Chromium and Chromium-Nickel Stainless Steel Plate, Sheet, and Strip for Pressure Vessels in ASME 2010

Section II Part A, SA-240 states that the code specification is "Identical with ASTM Specification A 240/A 240M-04."

The DCD, which was certified on May 12, 1997, states that the spent-fuel storage racks are purchased equipment. Not knowing when the racks will be procured, the DCD 9.1.3.3.2 states, "The racks are fabricated from materials used for construction, in accordance with the latest applicable ASTM specifications." Suppliers generally conform to the latest codes and standards in effect at the time of purchase. Consequently, at the time of procurement and fabrication, the codes and standards used, if later than those specified, will be reconciled to ensure that the codes and standards in effect meet or exceed those specified in the licensing requirements.

As stated above, Holtec Report No. HI-2135462, Section 2.3, Applicable Codes and Standards, Part a, Design Codes, will be revised to delete the references to "ASME B&PV Code Section III, Subsection NCA-3862, 2007 Edition," and "American Society for Nondestructive Testing SNT-TC-1A, "Recommended Practice for Personnel Qualifications and Certification in Nondestructive Testing", 2011 Edition" which are not used. References (5) and (6) will be designated "Deleted" as shown in gray shaded text below:

(4) ASME B&PV Code Section III, Subsection NF-3000 and NF-5000, 1989 Edition.

(5) Deleted.

(6) Deleted

Holtec Report No. HI-2135462, Section 2.3, Applicable Codes and Standards, will also be revised as shown by the gray shaded text below to clarify that at the time of procurement of the spent fuel racks, the codes and standards used by the supplier will be reconciled to ensure that the codes and standards in effect meet or exceed those specified in the licensing requirements:

2.3 Applicable Codes and Standards

The following codes, standards and practices are used, as applicable, for the design, construction, and assembly of the fuel storage racks. Unless a specific revision is identified in the list below, the latest revision is applicable. Suppliers generally conform to the latest codes and standards in effect at the time of purchase. Consequently, at the time of procurement and fabrication, the codes and standards used by the supplier, if later than those specified, will be reconciled to ensure that the codes and standards in effect meet or exceed those specified in the licensing requirements. Additional specific references related to detailed analyses are given in each section.

QUESTION:

Section 6.2.2, "Rack Acceptance Criteria," on Page 6-4, indicates an upward force of 13.35 kN for the stuck fuel assembly load case. However, Section 9.1.2.3.2 of STP 3 & 4 FSAR Revision 9 indicates that the rack is designed to withstand a pullup force of 17.79 kN and a horizontal force of 4.45 kN for the stuck fuel assembly load case. Correct the inconsistency or provide the technical basis for the use of upward force of only 13.35 kN and for ignoring the horizontal load of 4.45 kN.

RESPONSE:

ABWR Design Control Document (DCD) and the STP 3 & 4 FSAR, Section 9.1.2.3.2, Structural Design and Material Compatibility Requirements, Item (7), specifies that "The rack is designed to withstand a pullup force of 17.79 kN and a horizontal force of 4.45 kN." Verification that the spent fuel racks satisfy this requirement was verified as described in Letter U7-C-NINA-NRC-120071, dated November 14, 2013 (ML13326A573), Attachment 5, Item 3, and the information was incorporated into Holtec Report HI-2135462 as new Section 6.10, Stuck Fuel Assembly Evaluation.

Letter U7-C-NINA-NRC-120071, Attachment 5, Item 3, and Holtec Report HI-2135462, Section 6.10, included a reference to a DCD Chapter 9 requirement that the fuel racks must also withstand a "Postulated stuck fuel assembly causing an upward force of 13.35 kN." This requirement, which is less restrictive than "a pullup force of 17.79 kN and a horizontal force of 4.45 kN" was eliminated from the STP 3 & 4 FSAR by departure.

Holtec Report HI-2135462, Section 6.10, Stuck Fuel Assembly Evaluation, as presented in Letter U7-C-NINA-NRC-120071, Attachment 5, Item 3, will be revised as shown below:

6.10 Stuck Fuel Assembly Evaluation

The STP 3&4 spent fuel racks have been analyzed for a bounding vertical pull force of 17.9 kN (4,024 lb) plus a horizontal pull force of 4.45 kN (1,000 lb) applied simultaneously.

For the analysis, the stuck fuel assembly is postulated to occur at a corner cell location near the top of the rack, and the base of the rack is assumed to be fixed to the ground. This set of assumptions induces the maximum bending stress in the cellular region of the rack due to the vertical and horizontal pull forces. The stress calculations are performed manually using strength of materials formula. Specifically, the following stresses in the rack are evaluated:

a) the maximum tension plus bending stress in the rack cell cross section at the base of the cells (i.e., just above the base plate);

b) the maximum direct tensile stress on a single storage cell (assuming that the entire vertical pull force is resisted by a single cell);

c) the maximum shear stress in the cell-to-cell welds (assuming that the net resultant pull force is resisted by only two 6-inch long cell-to-cell welds);

d) the maximum shear stress in the adjacent base metal at the cell-to-cell weld locations.

In conjunction with this change, Holtec Report HI-2135462, Section 6.2.2 Rack Acceptance Criteria, will be revised to eliminate the reference to 13.35 kN in the statement to an "Upward force (13.35 kN)" in the following note in Table 6.1.1, Load Combinations and Acceptance Limits:

Pf = Upward force on the racks caused by postulated stuck fuel assembly

The results of the stuck fuel assembly analysis are summarized in the table below.

Result	Calculated Stress (psi)	Allowable Stress† (psi)	Safety Factor
Maximum tension plus bending stress in cell cross section	43.17	12,840	297
Maximum direct tensile stress on a single cell	2,180	12,840	5.89
Maximum shear stress in cell-to-cell welds	6,516	19,830	3.04
Maximum shear stress in base metal at cell-to-cell weld locations	4,607	8,560	1.86
† Allowable stresses are conservatively based on Level A service condition per ASME Section III, Subsection NF. Per Appendix D of SRP 3.8.4, the allowable stresses for Level B service condition can be applied to the stuck fuel assembly load.			

QUESTION:

Holtec Report No. HI-2135462, Section 2.3, "Applicable Codes and Standards," references Regulatory Guide (RG) 1.124, "Service Limits and Loading Combinations for Class 1 Linear-Type Component Support," Revision 1, which provides additional stress limits based on ultimate stress. These additional stress limits are not included in Holtec Report No. HI-2135462, Section 6.2.3, "Stress Limits for the "NF" Structure." Therefore, the staff requests that the applicant explain whether the stress limits in RG 1.124, Revision 1, were taken into account in the design of the fuel racks. If the stress limits in RG 1.124, Revision 1 were considered, then revise Holtec Report No. HI-2135462, Section 6.2.3, to include those requirements. If the stress limits were not considered, then provide the technical basis for not including them in the design calculations.

RESPONSE:

Holtec Report No. HI-2135462, Section 6.2.2, Rack Acceptance Criteria, Part b, Code Stress Limits under Different Service Conditions, will be revised to include the following:

The stress analysis of the spent fuel racks is consistent with all of the applicable guidance in NRC Regulatory Guide (RG) 1.124, Revision 1 for component supports designed by the linear elastic analysis method. Specifically, the seismic analysis of the spent fuel racks is consistent with guidance in RG 1.124, Revision 1 based on the following:

i) The value of S_y at temperature is less than 5/6 S_u for all structural materials specified for the STP 3&4 spent fuel racks.

ii) The compressive stress in the rack cell structure is demonstrated to be less than 2/3 of the critical buckling limit.

iii) There are no bolts or bolted connections anywhere in the spent fuel racks.

iv) Per the ABWR Design Control Document, OBE loading is not applicable to the STP 3&4 spent fuel racks.

v) For SSE load combinations, the calculated stresses in the spent fuel racks are compared with the stress limits of NF-3220 of Section III, increased according to the provisions of F-1334 of Section III.

In addition to the above, Holtec Report No. HI-2135462, Section 6.4.2, Essentials of the Dynamic Model, will be revised to note the following:

Figure 6.4.4 shows the modeling technique and degrees-of-freedom associated with rack elasticity. In each bending plane shear and bending springs simulate elastic effects [6.4.7]. Linear elastic springs coupling rack vertical and torsional degrees-of-freedom are also included in the model. It is noted that the lowest natural frequency of the rack cellular

structure, based on its mass and geometric properties, is approximately equal to the cut-off frequency of the input response spectra. Therefore, the rack cellular structure is essentially rigid, and the elastic deformations associated with the beam representation of the rack module are negligible. In other words, the maximum displacement of the rack at its top elevation is almost entirely the result of rigid body motion (i.e., sliding and rocking).

QUESTION:

Holtec Report No. HI-2135462, Section 6.2.3, "Stress Limits for the 'NF' Structure," presents stress limits for the design of the fuel racks. The report does not include the stress limits for tension and bending for the Level D condition. These limits cannot be determined by "the minimum of 2 or 1.167 Su/Sy times the corresponding Level A limits." Therefore, the staff requests that the applicant include the stress limits for tension and bending for the Level D condition in Holtec Report No. HI-2135462, Section 6.2.3, otherwise, provide the technical basis for not doing so.

RESPONSE:

The stress limits for tension and bending for the Level D condition are determined per Paragraph F-1334 of the ASME Code, Section III, Division 1 – Appendices, which states:

> "Unless otherwise specified, the allowable stresses presented (NF-3220) for Level A Service Condition may be increased using the following factors: the smaller of 2 or 1.167Su/Sy if Su > 1.2Sy, or 1.4 if Su ≤ 1.2Sy, where Sy is the yield strength, ksi (MPa), and Su is the ultimate tensile strength, ksi (MPa), both at temperature."

The following table summarizes the stress limits for tension and bending for Level A and Level D conditions for both construction materials. The allowable limits are expressed in units of psi.

Allowable Stress Limit	SA-240 304L		SA-564 630	
	Level A	Level D	Level A	Level D
Tension	12,840	25,680	63,780	98,030
Bending	12,840	25,680	63,780	98,030

The limit for combined axial tension and bending for the Level D condition is specified in Subparagraph F-1334.4 of the ASME Code, Section III, Division 1 – Appendices. Specifically, the following equation given in F-1334.4(a) must be satisfied:

$$\frac{f_a}{F_a} + \frac{f_{bx}}{F_{bx}} + \frac{f_{by}}{F_{by}} \leq 1$$

where F_a = smaller of $1.2S_y$ or $0.7S_u$. The necessarily unusual geometry of the rack does not allow the gross cross section to meet the compact section requirements of NF-3322.1(d), and therefore F-1334.4(b) is not applicable to the STP 3&4 spent fuel racks by strict code interpretation. For non-compact sections, F-1334.4(c) provides two methods for determining F_{bx} and F_{by}. The first method (i.e., F-1334.4(c)(1)) is overly conservative since it yields a value for F_b (= $0.523S_y$) that is less than the allowable bending stress for box-type flexural members *for Level A conditions* ($0.6S_y$). The second method (i.e., F-1334.4(c)(2)), which is applied to the

STP 3&4 spent fuel racks, calls for a rigorous analysis of member stability to determine the allowable design bending stress. As described in the response to RAI 09.01.02-64, a stability analysis of a 3x3 cell array has been performed using ANSYS to demonstrate that the maximum compressive stress in the cells due to combined bending plus axial load is less than the critical buckling stress by at least a factor of 1.5. This analysis satisfies the intent of F-1334.4(c)(2) and shows that the combined tension and bending stress in the rack cell structure is acceptable.

Holtec Report HI-2135462, Section 6.2.3.1.2, Level D Service Limits, will be revised to add the following shown as gray shaded text:

6.2.3.1.2 Level D Service Limits

Section F-1334 (ASME Section III, Appendix F) [6.2.6], states that the limits for the Level D condition are the minimum of 2 or 1.167 S_u/S_y times the corresponding limits for the Level A condition if $S_u > 1.2S_y$, or 1.4 if $S_u \leq 1.2S_y$ except for requirements specifically listed below. S_u and S_y are the ultimate strength and yield strength, respectively, at the specified rack design temperature.

The construction materials used to build the spent fuel racks are SA-240 304L and SA-564 630 (age hardened at 1100F), as shown in Table 6.5.1. Based on the strength values given in Table 6.5.1, Su > 1.2Sy for SA-240 304L and SA-564 630. Therefore, the increase factor for both materials is the smaller of 2 or 1.167Su/Sy. For SA-240 304L, the factor of 2 controls. For SA-564 630, 1.167Su/Sy (= 1.537) is the controlling factor.

Exceptions to the above general multiplier are the following:

a) Stresses in shear shall not exceed the lesser of $0.72S_y$ or $0.42S_u$. In the case of the austenitic stainless material (SA 240-304L), $0.72S_y$ governs. For the lower part of the support pedestal (SA 564-630), $0.42S_u$ governs.

b) Axial Compression Loads shall be limited to 2/3 of the calculated buckling load.

c) Combined Axial Compression and Bending - The equations for Level A conditions shall apply except that:
F_a = 0.667 × Buckling Load/ Gross Section Area,
and the terms F'_{ex} and F'_{ey} may be increased by the factor 1.65.

d) Combined Axial Tension and Bending - The following equation shall be satisfied:

$$\frac{f_a}{F_a} + \frac{f_{bx}}{F_{bx}} + \frac{f_{by}}{F_{by}} \leq 1$$

where F_a = smaller of $1.2S_y$ or $0.7S_u$. Consistent with F-1334.4(c)(2), F_{bx} and F_{by} are determined from a rigorous analysis of the cell wall stability (see Section 6.7.10). The allowable bending stresses (F_{bx} and F_{by}) are conservatively set to 8,200 psi based on the analysis results.

e) For welds, the Level D allowable maximum weld stress is not specified in Appendix F of the ASME Code. An appropriate limit for weld throat stress is conservatively set here as:

$F_w = (0.3\ S_u) \times$ factor

where:

factor = (Level D shear stress limit)/(Level A shear stress limit)

$= 0.72 \times Sy / 0.4 \times Sy = 1.8$

Finally, it is noted that many of the rack components are fabricated using material that is dual certified as SA-240 304/304L, which means that the strength properties of the material meet or exceed the minimum strength requirements for SA-240 304 and SA-240 304L. For conservatism, the stress analysis of the racks is performed using the lesser properties of SA-240 304L, except where noted.

QUESTION:

Holtec Report No. HI-2135462, Section 6.7.1, "Fuel Rattling Loads," discusses the calculation of the maximum g-load that the rack imparts to the fuel assembly. The report states:

The bounding fuel-to-cell wall impact load, at any level in the rack, for all runs is less than or equal 1,774 lb (see Table 6.6.1). For the five lumped mass model (with 25% at the ¼ points and 12.5% at the ends), the maximum g-load that the rack imparts on the fuel assembly can be computed as:

$$a = \frac{4F}{w} = 10.51g$$

where: a = maximum lateral acceleration in g's
F = maximum fuel-to-cell wall impact force (= 1,774 lbf)
w = weight of one fuel assembly (conservatively taken to be 675 lbf)

The staff requests that the applicant identify where the maximum impact load (1,774 lbs) occurs, i.e., at the top of the fuel assembly or at an intermediate height. If the maximum impact load occurs at the top, where only 12.5% of the mass is assumed at the ends of the fuel assembly, the factor in the equation for the g-load should be 8 instead of 4. If the maximum impact load occurs at an intermediate height, where 25% of the mass is assumed, then 4 is correct; however, the top should also be checked, using 8 instead of 4 in the equation to determine which calculation results in the highest g-load. The staff requests that the applicant provide additional results based on the top location, or provide the technical basis explaining why the use of a factor of 4 is always correct.

RESPONSE:

The maximum impact load (1,774 lbf) occurs at an intermediate height, where 25% of the mass is assumed. Therefore, the factor of 4 is correct in the above formula. The maximum impact load at the top of a fuel assembly is 1,251 lbf (see RAI 09.01.02-60). To address both impact locations, HI-2135462 Section 6.7.1, Fuel Rattling Loads, and Section 6.12, References, will be revised as shown below.

6.7.1 Fuel Rattling Loads

6.7.1.1 Fuel Impact Loads

The bounding fuel-to-cell wall impact load, at any level in the rack, for all runs is less than or equal to 1,774 lb (see Table 6.6.1.b). This impact load occurs at an intermediate height location (i.e., node location 3*, 4*, and 5* in Figure 6.4.1). The maximum impact load at the top or bottom end of the fuel assembly (i.e., node locations 1* and 2* in Figure 6.4.1) is 1,251 lb [6.7.10]. For the five lumped mass model (with 25% at the 1/4 points and 12.5% at the ends), the maximum g-load that the rack imparts on the fuel assembly can be computed as the maximum of:

$$a = \frac{4F_{mid}}{w} = 10.51g$$

$$a = \frac{8F_{end}}{w} = 14.83g$$

where: a = maximum lateral acceleration in g's
F_{mid} = maximum fuel-to-cell wall impact force at intermediate node (= 1,774 lbf)
F_{end} = maximum fuel-to-cell wall impact force at end node (= 1,251 lbf)
w = weight of one fuel assembly (conservatively taken to be 675 lbf)
Note: w/4 = 25% of the weight of one assembly; w/8 = 12.5% of weight of one assembly.

6.7.1.2 Fuel Acceptance Criteria

The lateral impact loads on the spent fuel assemblies, which result from the fuel rattling inside the rack storage cells during an earthquake, is evaluated against three acceptance criteria:

Fuel cladding yield stress,
Fuel cladding strain, and
Fuel spacer grid buckling.

NUREG/CR-1864, "A Pilot Probabilistic Risk Assessment of a Dry Cask Storage System at a Nuclear Power Plant", provides temperature-dependent mechanical properties for the Zircaloy cladding material which were obtained from PNNL data on high-burnup fuel [6.7.6].

Elastic Modulus = 11.0×10^6 psi
Yield Strength = 92.4×10^3 psi
Yield Strain = 0.0084 in/in

Sandia Report SAND90-2406 [6.7.7] provides an analysis which predicts the onset of buckling of the BWR spacer grid at 75.7 N (17 lbf) of load per fuel rod.

The spent fuel assemblies are not expected to suffer any damage while stored inside the spent fuel storage racks because the lateral impact loads that occur inside the spent fuel storage racks are much smaller than the impact loads associated with transportation casks licensed under 10 CFR 71. For example, the HI-STAR 100 transport cask is qualified for a 9-meter drop accident resulting in a 60 g impact load [6.7.8].

The following analyses will demonstrate that the fuel spacer grid does not buckle and that the fuel rod cladding is well below limits of failure.

6.7.1.3 Buckling Evaluation of Fuel Spacer Grid

The lateral impact load on a single fuel grid spacer is compared against its buckling capacity, which is derived from the data in Sandia Report SAND90-2406.

The initial loading from the fuel rods during a lateral impact compresses the leaf springs onto the spacer grid frame. Further loading after the spacer contact springs bottom out results in deflection of the spacer frame. The spacer grid frames provide resistance to the point where the frame begins to buckle. After buckling, the frame offers minimal resistance to further load. The objective of this analysis is to demonstrate that the spacer grids do not buckle and consequently rod-to-rod contact does not occur. Rod-to-rod contact would produce crushing loads on the rods and require further analysis.

The Sandia fuel assembly spacer grid model for the GE 7 X 7 fuel assembly is based on the assembly spacer-grid nonlinear spring element obtained from the analysis of a single spacer grid cell. The basis of this cell model was verified through extensive modeling of entire spacer grid frames, as described in the report. The spacer grid nonlinear spring elements developed are illustrated in the Sandia report.

The Sandia report shows the deflected shape from the GE 7x7 single-bay slice model analysis and the force deflection spring elements developed for the example BWR assembly models used to simulate the spacer grids for the two-dimensional side drop assembly analyses.

Each spring element will accrue the force from all rods adjacent to the spring of interest, and so the buckling force of 454 N (102 lbf) for an individual cell is equivalent to a force of 75.7 N in each rod that buckles the last cell in the row (454 N is equal to six rods multiplied by 75.7 N per rod).

Although the Sandia report does not provide specific results for a GE 8X8 fuel spacer grid, the load limit for a GE 8X8 fuel spacer grid can be derived from the GE 7X7 results, since

the spacer grid materials and construction are essentially the same, except the individual cells are smaller to accommodate the larger array.

The buckling capacity of the spacer grid is inversely proportional to the square of the cell size, i.e., the length of the unsupported "column", and the cell size is directly related to the fuel rod pitch. Since the cells in the 8X8 spacer grid are smaller than the 7X7 spacer grid, the smaller cells are more resistance to buckling.

$$\text{Ratio} = \frac{\text{P7x7}}{\text{P8x8}} = \frac{1.8745cm}{1.6256cm} = 1.153$$

Therefore, critical buckling load for the 8X8 fuel spacer grid is (102 lbf)$(1.153)^2$ = 135.6 lbf.

Furthermore, in this assessment, the mass of the fuel assembly channel does not contribute to the buckling loads on the spacer grid, so only the fuel rod mass is considered in this analysis.

From Table C.1 of NUREG-1864, the cladding mass is 1.70 lbm, and the fuel mass is 7.46 lbm, or

$$\frac{1.70 + 7.46}{144} = 0.0636 \text{ lbm}/in.$$

The load imposed on a cell in the spacer grid is ½ the mass of the fuel rod on each side of the spacer cell or 2 (19.62/2 in)(0.0636 lbm/in)(14.83 g) = 18.50 lbf, and the combined load from 7 fuel rods adjacent to the critical cell is 7 X 18.50 = 129.5 lbf.

Therefore, the safety factor against buckling is 135.6 lbf/129.5 lbf = 1.047. The calculated safety factor is conservative since the buckling evaluation of the grid spacer does not take any credit for the fuel channel, which surrounds the grid spacers and increases their buckling capacity. In addition, the buckling evaluation uses the maximum impact deceleration at the top of the stored fuel assembly; however, there are no grid spacers at the top or bottom lumped mass lengths.

6.7.1.4 Stress/Strain Evaluation of Fuel Cladding

The fuel mass acceleration is used to calculate a load uniformly distributed over a single fuel rod modeled as a beam simply support by the spacer grids 19.62 inches apart.

As stated above, the fuel assembly channel mass does not contribute to the bending loads on the fuel rods.

The uniformly distributed load is:

$$q = a \times w_{fuel} = 14.83 \times 0.0636 \text{ lbm/in} = 0.943 \text{ lbf/in}$$

The maximum bending moment is:

$$M = (w_{fuel} \times L_{spacer}^2)/8 = (0.943)(19.62)^2/8 = 45.37 \text{ lbf-in}$$

The resulting maximum bending stress in the fuel cladding is 9,460 psi.

Compared to the yield stress of 92.4×10^3 for irradiated Zircaloy, the resulting factor of safety is 9.77.

The strain associated with this maximum stress is $\epsilon = \sigma/E = 0.0008$ in/in which is well below the yield strain of 0.0084 in/in for irradiated Zircaloy.

In summary, the bending stress (9,460 psi) induced in the fuel rod cladding due to the maximum lateral acceleration, a, is well below the yield strength of Zircaloy cladding (92,400 psi), and the strain (0.0008 in/in) is well below the yield strain (0.0084 in/in). Finally, the maximum computed impact load on an individual fuel grid spacer cell (129.5 lbf) is less than its buckling capacity (135.6 lbf). Therefore, the structural integrity of the stored fuel assemblies under an SSE event is assured.

6.7.1.5 Bending Stress in Fuel Channel

The maximum clearance between the cell walls and the outside envelope of the channeled fuel assembly is 0.52". Thus, to obtain an upper bound estimate of the bending stress that could develop in the fuel channel during an earthquake, the fuel channel is considered as a simply supported beam subjected to a lateral deflection of 0.52" at its midspan. The bending stress in the fuel channel due to this loading condition is 6,072 psi, which is much less than the yield strength of Zircaloy (92,400 psi). Since the bending stress in the fuel channel remains well within the elastic range, the fuel channel will not suffer any damage as a result of a design basis earthquake.

6.12 References

[6.7.6] Geelhood, K.J., and C.E. Beyer, "Mechanical Properties of Irradiated Zircalloy," Transactions of ANS Winter Meeting, Vol 93, American Nuclear Society, Washington, DC, November 2005.

[6.7.7]. Sandia Report SAND90-2406, "A Method for Determining the Spent-Fuel Contribution to Transport Cask Containment Requirements", November 1992

[6.7.8] HI-951251 Safety Analysis Report on the HI-STAR100 Cask System, Rev. 15.

[6.7.9] Timoshenko, S.P and Gere, J., Theory of Elastic Stability, McGraw-Hill Book Company, Second Edition.

[6.7.10] Holtec Report HI-2135615, Structural/Seismic Analysis of Fuel Racks at South Texas Project, Units 3 & 4, Rev. 3.

QUESTION:

NINA Letter, U7-C-NINA-NRC-130059, dated November 14, 2013, Attachment 5, Item 3 provides stuck fuel assembly evaluation required by the ABWR DCD, Subsection 9.1.2.3, but is not currently included in Holtec Report No. HI-2135462. In light of the information in Item 1, Figure 2.11, which shows that the cell-to-cell welds are 8 inches long, explain the assumption "that the net resultant pull force is resisted by only two 6-inch long cell-to-cell welds [...]," which is found in Item 3c) of Attachment 5.

RESPONSE:

The minimum cell-to-cell weld length is 6 inches as shown on Sheet 4 of Holtec Drawing 8946. In order to form this weld, an 8-inch long tie bar is positioned between the opposing corners of the cells being welded at each cell-to-cell weld location. The tie bar length is 2" longer than the minimum required weld length to avoid potential weld issues at the ends of the tie bar. Figure 2.11 shows the length of the tie bar, but it does not indicate the minimum cell-to-cell weld length.

Holtec Report HI-2135462, Figure 2.11, Tie Bar Weld Details, will be revised as shown on the following page to include the details described above.

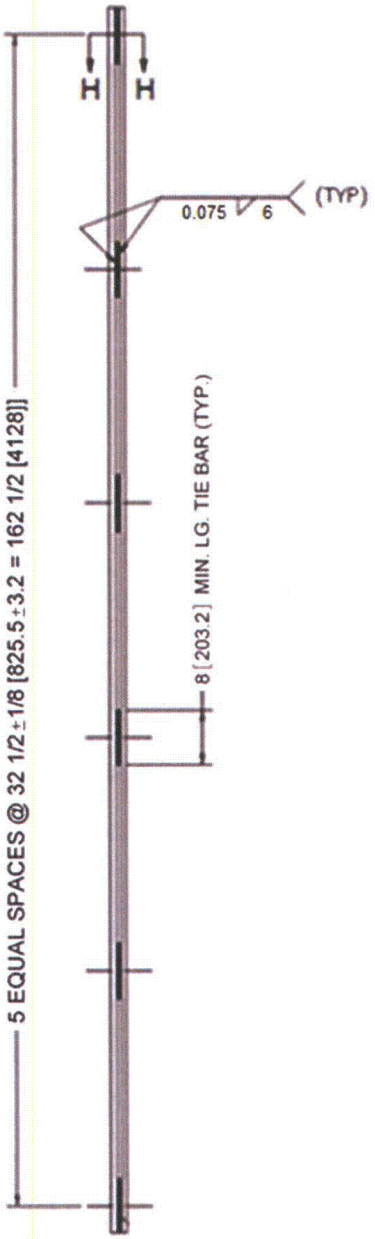

FIGURE 2.11: TIE BAR WELD DETAILS

QUESTION:

NINA Letter, U7-C-NINA-NRC-130059, dated November 14, 2013, Attachment 5, Item 4 discusses the consideration of "out-of-phase movement of fuel assembly for determining maximum impact force on fuel assembly." The response referenced a full scale model test on a shaker table and indicated that the test results clearly show that the fuel assemblies rattle in unison. The staff requests that the applicant update Holtec Report No. HI-2135462 to document the basis for not considering out-of-phase movement of the fuel assembly in the determination of maximum impact force on the fuel assembly.

RESPONSE:

The following will be added to Holtec Report HI-2135462, Section 6.4.2, Essentials of the Dynamic Model, part b:

> It is highly unlikely, if not impossible, that two adjacent fuel assemblies move 180° out of phase towards each other such that they impact the cell wall at precisely the same instant in time at the same vertical location. Fuel assemblies are much more likely to rattle in unison, like multiple clappers in a bell. A Japanese study constructed a full-scale free-standing spent fuel rack loaded with fuel assembly masses. The full scale model was tested on a shaker table to record the seismic response of the rack and fuel assemblies. The test results clearly show that the fuel assemblies rattle in unison, thereby justifying the accepted analytical practice of modeling all the fuel assemblies in a rack as a single large segmented mass [6.4.8].

In addition, Holtec Report HI-2134562, Section 6.12, will be revised to include the following reference:

[6.4.8] Proceedings of the ASME 2012 Pressure Vessels & Piping Conference, PVP2012-78451, "Experimental Study on Free Standing Rack Loading Full Fuel Assembly", July 15-19, 2012, Toronto, Ontario, Canada.

09.01.02-48

QUESTION:

NINA Letter, U7-C-NINA-NRC-130059, dated November 14, 2013, Attachment 5, Item 5 discusses evaluation of cell-to-cell welds. The response stated that the stresses in the welds arising from fuel assembly impacts with the cell wall are calculated assuming the fuel assemblies in the adjacent cells move out of phase, and that the stresses arising from shear flow in the rack cross section are based on maximum computed R2 and R7 stress factors. However, the response did not provide any description of how the stresses in the welds are calculated for the two loadings above. Since the weld stress calculations are not based on a detailed model of the honeycomb rack design and use simplifying assumptions, details of the methodology used for determination of weld stresses due to fuel impact load and shear flow are needed for the staff to determine whether the evaluation is acceptable. The applicant is requested to:

(1) provide details of how the stresses in cell-to-cell welds are determined, including calculation of demand, the cell wall impact area assumed, and the weld length used; and

(2) explain how loads are transferred through tie bars by showing a free-body diagram of tie bar.

RESPONSE:

(1) & (2) This response includes as attachment 16 A, an excerpt from Holtec Report No. HI-2135615, which provides the details of how the stresses in the cell-to-cell welds due to fuel impact load and shear flow are determined. It is noted that calculations in this excerpt have been updated based on feedback from the NRC Staff during the February 4-5, 2014 audit at the Westinghouse Twinbrook office in Rockville, Maryland and the March
3-7, 2014 audit at the Holtec office in Marlton, NJ. This excerpt includes a free-body diagram showing how the impact loads are transferred through the tie bars.

With regard to the R2 and R7 shear factors, which are defined in Section 6.2.3.2 of Holtec Report No. HI-2135462, these factors are calculated based on the gross cross sectional area of the rack cell structure. For conservatism, the calculated R2 and R7 shear factors have been increased by a factor of 2 so that only the cell walls parallel to the direction of the shear load are considered effective in resisting shear. As a result of this change, the minimum required length for each individual cell-to-base plate weld has been increased from 4" to 4.5".

Holtec Report HI-2135462, Section 6.7.9 (parts a and c), will be revised as shown by the gray shaded text below:

a. Baseplate-to-Rack Cell Welds

The rack's cellular structure is connected to the base plate through fillet welds that are 4.5 inches long. The maximum values of the tensile stresses in the connecting welds and the adjacent base metal are computed using the maximum values of the stress factors from the DYNARACK simulations.

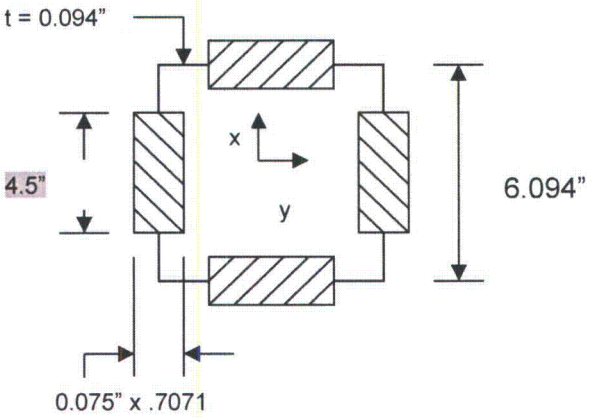

Weld stresses (see figure above) are determined through the use of a conversion factor (based on area ratios) applied to the corresponding stress factor in the adjacent rack material.

For SFR,

$$\frac{0.094*(6+0.094)}{0.075*0.7071*4.5}=2.4$$

0.094"	is the cell wall thickness
6"+0.094"	is the mean box dimension
0.075"*0.7071"	is the box-baseplate fillet weld throat size
4.5"	is the minimum length of the weld

The highest predicted cell to baseplate weld stress is calculated based on the highest R6 value for the rack cell region tension stress factor and R2 and R7 values for the rack cell region shear stress factors (refer to subsection 6.2.3.2 for definition of these factors). The R2 and R7 stress factors are conservatively multiplied by a factor of 2 so that only the cell walls parallel to the direction of shear load are effective in resisting shear. These cell wall stress factors are converted into weld stress values as follows:

For SFR SSE Simulation

$\{[R6 * (1.2)]^2 + [2 * R2 * (0.72)]^2 + [2 * R7 * (0.72)]^2\}^{1/2} * S_y * Ratio$

$= \{[0.319 * (1.2)]^2 + [2 * 0.101 * (0.72)]^2 + [2 * 0.115 * (0.72)]^2\}^{1/2} * (21,400) * 2.4$

$= 22,686$ psi

The above calculation is conservative because the maximum stress factors used above do not all occur at the same time instant. The table below shows the stress in weld and base metal along with the associated factors of safety (allowable is 1.0 minimum).

	Stress (psi)	Allowable stress (psi)	Safety Factor
Weld	22,686	35,694	1.57
Base Metal	16,041	18,000[‡‡]	1.12

c. Cell-to-cell welds

Cell-to-cell joints consist of a series of connecting welds along the cell height. Stresses in storage cell to cell welds develop due to (i) fuel assembly impacts with the cell wall and (ii) shear flow in the rack cross section resulting from beam-type flexure. The weld stresses arising from (i) are conservatively calculated by considering that fuel assemblies in adjacent cells are moving out of phase with one another so that impact loads in two adjacent cells are in opposite directions thus maximizing the stress in the connecting longitudinal welds. The weld stresses arising from (ii) are determined based on the geometric properties of the gross cell cross section and the maximum horizontal shear forces acting on the rack cell structure in the x- and y-directions. The weld stress contributions from (i) and (ii) are combined to obtain the maximum cell-to-cell weld stress. Both the weld and the base metal shear stress results using this approach are summarized below:

Analysis Type	Stress (psi)	Allowable stress (psi)	Safety Factor
Weld	22,082	35,694	1.62
Base Metal	15,614	18,000[§§]	1.15

QUESTION:

NINA Letter, U7-C-NINA-NRC-130059, dated November 14, 2013, Attachment 5, Item 6 discusses the design check for rack cell wall, base plate, and bearing plate. In order for the staff to complete its review, the applicant is requested to provide the following additional information:

(1) Regarding the analysis of fuel to cell wall impact, a plastic analysis of the cell wall is described. The staff notes that Holtec Report No. HI-2135462, Section 6.7.5, "Storage Cell Deformation," states that the primary stresses are within the elastic limit and plastic deformation of the cell wall from rattling action is ruled out. This appears to contradict the analysis methodology described in the response. Therefore, the staff requests that the applicant explain the inconsistency identified and provide the technical basis for the analysis method described in the Item 6 response. Also, the response states that the allowable impact load is taken as 50% of the limit load (QL). Explain how the stress limits presented in Holtec Report No. HI-2135462 Section 6.2.3, "Stress Limits for the 'NF' Structure," are satisfied. If not satisfied, provide the technical basis. In addition, provide the assumed effective width of the cell wall and its basis. Also, explain why two load points were considered. Additionally, provide the distance between the load points and its basis, and explain whether fuel disposition (e.g., rotation and off from halfway between the cell walls) needs to be considered in the determination of the load points.

(2) Regarding the buckling analysis of the cell wall subject to rack-to-rack impact, the proposed changes to Holtec Report No. HI-2135462 state that the impact load is applied to the back surface of the rigid impactor as a uniform pressure across the full width of the rack. The staff requests that the applicant provide the technical basis for the assumption of the uniform pressure across the full width of the rack. Additionally, explain why the impact force time history was amplified to have a peak force of 557 kips, and how the displacement time history of the impactor was computed.

(3) Regarding the base plate design check, the response states that the compressive stress on the baseplate due to rack-to-rack impacts is discussed in Holtec Report No. HI-2135462, Section 6.7.6, "Rack-to-Rack and Rack-to-Wall Impacts." The staff requests that the applicant explain whether other stresses such as bending and shear stresses due to support reactions, as well as the combination effect, were also checked. If other stresses were checked, then provide the detailed design check. If other stresses were not checked, then provide the technical basis for not performing the check.

(4) Regarding the concrete bearing stress evaluation, Holtec Report No. HI-2135462, Section 6.9, "Qualification of the Bearing Pad and Bearing Pressure on the Pool Slab," indicates the entire bearing pad area was used to calculate the bearing stress. Since the bearing pad is described as a shim plate under compression, the staff requests that the applicant provide the technical basis for assuming that the bearing pad applies a uniform bearing stress in the concrete over the entire bearing pad area (18"x18").

(5) Update the report HI-2135462, as necessary, to include the information requested above.

RESPONSE:

(1) Per Appendix D of SRP 3.8.4, the spent fuel racks are designed and analyzed as Class 3 component supports per ASME Code, Section III, Division 1, Subsection NF. As such, the rack cell structure is considered as a beam type member, and the stress limits for NF structures in Section 6.2.3 are only applied to the primary stresses acting on the gross cell cross section. The fuel-to-cell wall impacts produce local stresses in the cell wall, which are not subject to the primary stress limits given in Section 6.2.3. In order to ensure that the fuel-to-cell wall impacts do not cause significant plastic deformation, which may affect the sub-criticality of the stored fuel array, a limit analysis is performed to establish the maximum fuel-to-cell impact load that can be sustained without exceeding the ultimate moment capacity of the cell wall while maintaining a factor of safety of 2. Based on this approach, the maximum allowable impact load is determined to be 3,636 lbf (as compared to a maximum predicted impact load of 1,774 lbf).

If the maximum predicted impact load of 1,774 lbf is used to calculate the bending stress in the cell wall (using the same beam model as described in Item 6 of NINA Letter, U7-C-NINA-NRC-130059, Attachment 5), then the maximum bending stress is 14,981 psi, which is well below the minimum yield strength (25,000 psi) of the dual certified SA-240 304/304L material at 200°F. This is the basis for the statement in Section 6.7.5 of HI-2135462, which reads: "Classical strength of materials calculations show that the primary stresses in the cell wall under the lateral impact load from the rattling of the fuel assemblies remain in the elastic range."

The effective length of the cell wall used in the above calculations is 10 inches. Since the cell wall is treated as a one-way beam strip, there is no credit taken for the load resistance from the continuous cell wall beyond the 10-inch length. This length is conservative based on the fact that BWR fuel assemblies have 7 fuel grid spacers over a 146 inch active fuel length, so the length attributable to each fuel grid spacer is approximately 18.25 inches (= 146 / (7+1)). Also, the DYNARACK model assumes only 5 fuel masses equally spaced over the cell height (171"), which means that each intermediate fuel mass has a tributary length of 42.75 inches. Since this length encompasses at least 2 fuel grid spacers, it is conservative to apply the maximum predicted impact load over a 10 inch cell length. Finally, it is noted that the stresses in the cell wall would remain elastic even if the effective length of the cell wall was reduced to as low as 6 inches.

The spacing between the load points is equal to the OD of the fuel assembly (5.48") since the impact load will shift to the corner edges of the fuel assembly during an impact. Considering the conservative value used for the effective cell width and the fact that the calculations show a safety factor of more than 4 against the limit load, there is enough embedded margin that the disposition of the fuel need not be considered.

Section 6.7.5 of Holtec Report No. HI-2135462 will be updated as follows:

> Even though limits on secondary stresses are not prescribed in the ASME Code for Class 3 NF structures, analysis has been performed in support of this safety evaluation to insure that the localized impacts do not lead to significant plastic deformations in the storage cell walls which may affect the sub-criticality of the stored fuel array. In fact, classical

strength of materials calculations show that the primary bending stress in the cell wall under the maximum lateral impact load from the rattling of the fuel assemblies remains below the yield strength of the cell wall material. Thus, a plastic deformation of the cell wall from the rattling action of fuel during a seismic event is ruled out.

(2) The impact load is applied across the full width of the rigid impactor since the DYNARACK solution indicates that both end of the bumper bar (along the side of the rack) are in contact when the maximum rack-to-rack impact load occurs. The impact force time history, which is obtained from the dynamic simulation of the spent fuel racks using DYNARACK, is amplified by a factor of 3 to demonstrate that the critical buckling load is at least 1.5 times greater than the maximum predicted impact load. The displacement time history of the impactor is computed by LS-DYNA based on the geometry and strength properties of the rack and the impact force time history.

The maximum calculated impact load of 188,780 lbf is based on a rack-to-rack impact spring rate of 431,000 lbf/in at each corner. This spring rate is calculated assuming that the impact load is resisted only by the two perimeter cell walls over a depth that is equal to 3 times the cell inner dimension. In order to assess the sensitivity of the rack-to-rack impact load to the spring rate, two sensitivity runs have been performed in which the spring rate is increased. In the first run (Run No. 28), the spring rate is calculated assuming that the impact load is resisted by six cells (3 per corner) over a depth that is equal to one half of the rack width. The resulting spring rate is 517,000 lbf/in, which is roughly 20% greater than the original spring rate. When this value is used, the maximum impact load increases by 6.2% to 200,540 lbf. In the second sensitivity run (Run No. 29), the original spring rate is increased by 50% to 646,000 lbf/in, which caused the impact load to increase by 11.5% to 210,480 lbf. The results from these two runs show that the impact load is starting to plateau (i.e., the increase in impact load is diminishing as the spring rate increases). This can be observed from the following graph.

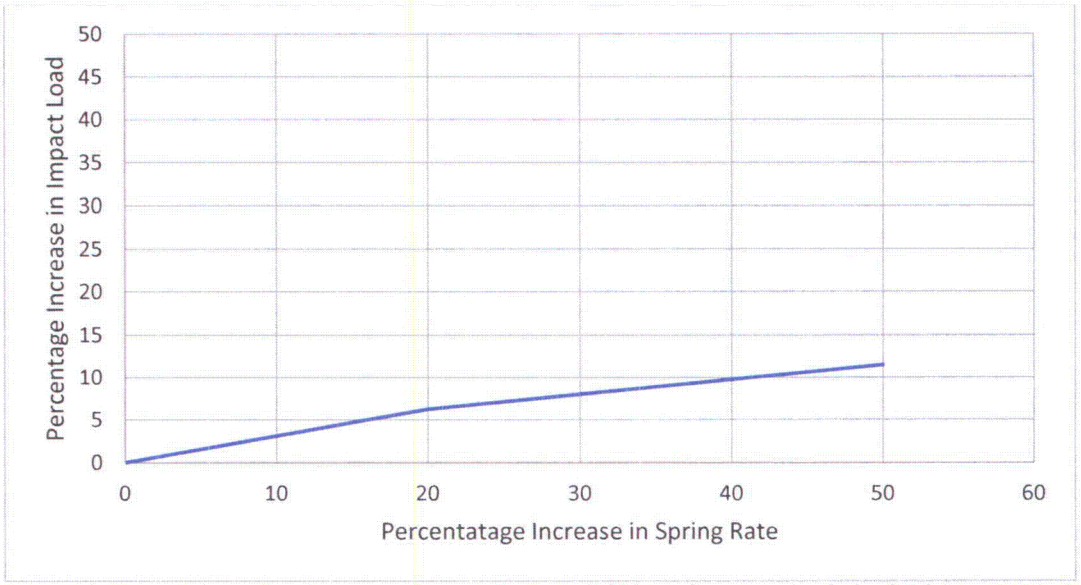

The maximum impact load of 210,480 lbf is less than two-thirds of the critical buckling capacity of the spent fuel rack based on the rack-to-rack impact analysis performed using LS-DYNA. The critical impact load from the analysis is 339,420 lbf, which means that the allowable impact load is 226,280 lbf (= 2/3 x 339,420 lbf). Therefore, the rack design is structurally adequate to withstand the maximum rack-to-rack impact load.

HI-2135462 Section 6.7.6, Rack-to-Rack and Rack-to-Wall Impacts, will be revised to read as follows (which supersedes Item 6 from NINA Letter U7-C-NINA-NRC-130059, Attachment 2):

In order to protect the rack cellular structure from impact during a seismic event and maintain the installed inter-rack spacing, the rack baseplates extend beyond the perimeter envelope of the cell region. The racks are then installed in the pool with minimum gap between the contiguous baseplate edges. Therefore, by design the racks are predisposed to impact each other at the baseplate level during a seismic event, rather than at the top of rack elevation. The thick baseplates used in the rack modules are thus subject to sporadic impact loads during the earthquake.

Results from the dynamic analysis indicate rack-to-rack impacts at the top as well as at the baseplate locations. 0.5" thick bumper bars are located at the top of the racks (on all 4 sides) to mitigate the rack-to-rack impact load and reinforce the rack cell structure. The maximum impact load at the top from among all runs is 210,500 lbf (across the full width of the rack).

The ability of the rack to withstand the maximum rack-to-rack impact load is analyzed using the Holtec QA validated commercial finite element code LS-DYNA. The objective of the analysis is to demonstrate that the rack cell structure will not buckle under 1.5 times the maximum impact load, as required by Section III, Appendix F, F-1331.5 of the American Society of Mechanical Engineers (ASME) code. Figure 6.7.4 shows the LS-DYNA model used to evaluate the impact capacity of the rack. The LS-DYNA model takes advantage of the symmetry of the impact problem by applying appropriate boundary conditions and adjusting the cell wall thickness at the symmetry plane. As shown in the model, the top of the impacted rack is in contact with an 8" wide rigid rectangular plate, which represents the impactor (i.e., the adjacent rack) in a rack-to-rack impact event. The bounding impact force time history, which is obtained from the WPMR analysis and further amplified by almost a factor of 3 (such that it has a peak value of 557 kips), is applied to the back surface of the rigid impactor as a uniform pressure. Figure 6.7.5 shows the impact force time history applied to the rack top. The displacement time history of the impactor for the analyzed rack-to-rack top impact is presented in Figure 6.7.6, which shows no sudden increase until 0.017 seconds when the impact force reaches 339.4 kips. At the time that the maximum impact load (210.5 kips)

is reached, there is no permanent deformation in the rack cells. Based on the amplified input impact force time history shown in Figure 6.7.5, the safety factor against buckling is determined as follows.

Impact Force at Buckling	Maximum Impact Force	Safety Factor
339.4 kips	210.5 kips	1.61

The calculated safety factor against buckling is obtained by dividing the impact force at the onset of buckling with the peak impact force experienced by the rack during the SSE event. The calculated safety factor of 1.61 exceeds the minimum required value per Subsection NF of the ASME Code. Therefore, the rack design can safely withstand the maximum rack-to-rack impact load.

The maximum impact load at the baseplate from among all runs is 226,420 lbf (across the full width of the rack). The compressive stress due to the maximum impact at the baseplate is 2,668 psi, which is very low compared to the yield strength of the base metal material (21,400 psi).

There are no rack-to-wall impacts due to the seismic loadings.

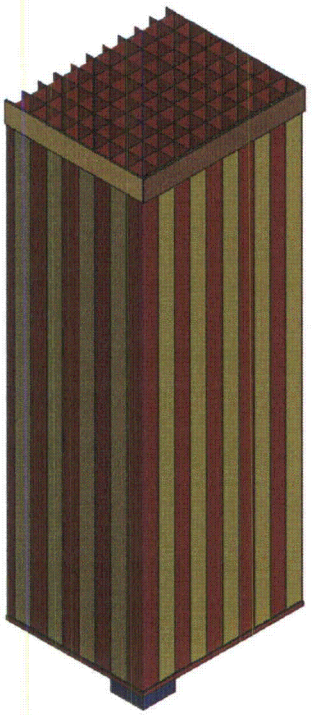

Figure 6.7.4 – Rack-to-Rack Impact LS-DYNA Model

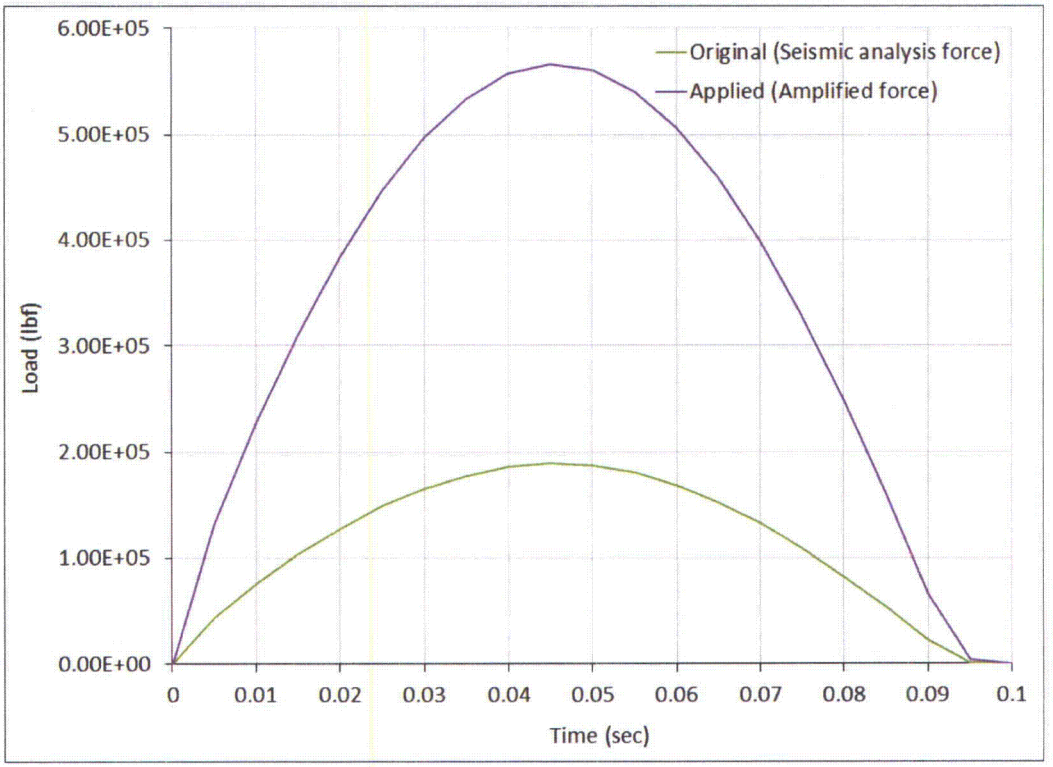

Figure 6.7.5 – Force Time History for Rack-to-Rack Impact Analysis

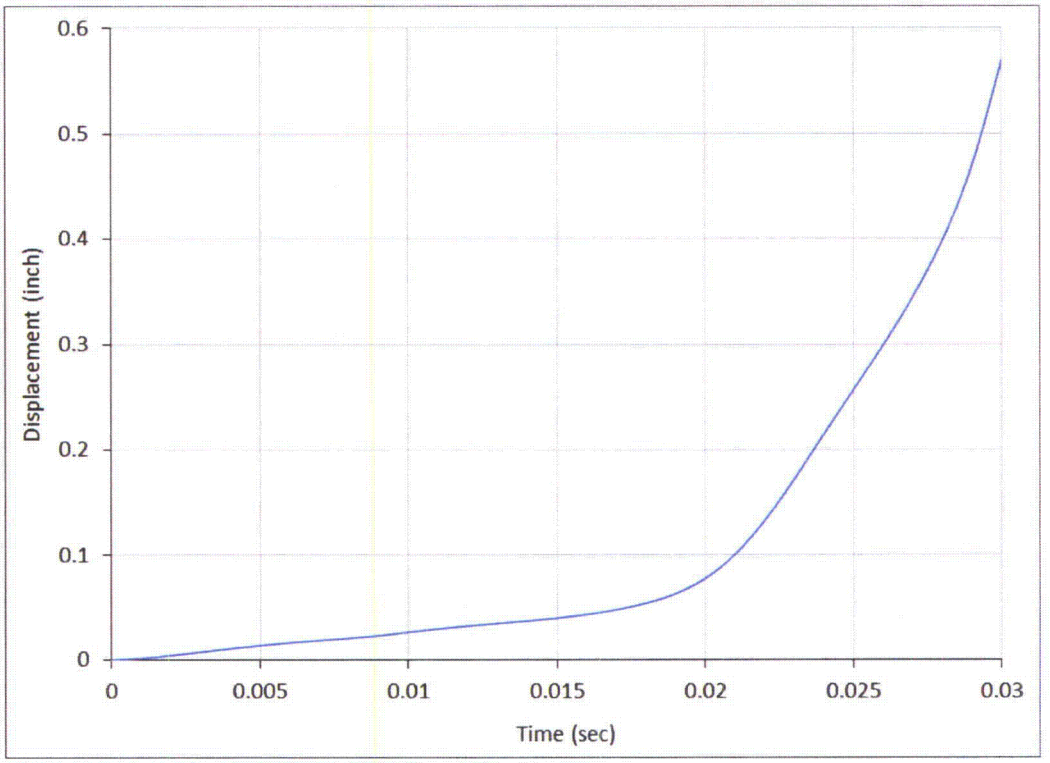

Figure 6.7.6 – Displacement Time History of the Impactor

(3) A punching shear evaluation of the rack base plate under the maximum support load has been performed. Bending stresses in the base plate are not significant since each storage cell is welded to the top surface of the base plate creating a highly rigid structure.

(4) In order to insure that the bearing stress in the concrete is below the allowable limit, the bearing pad thickness will be increased from 2" to 2-1/2", and the bearing stress calculation will be revised to credit only a 13" diameter contact area.

Holtec Report HI-2135462, Section 6.9, Qualification of the Bearing Pad and Bearing Pressure on the Pool Slab, will be revised to reflect these changes and the changes described in RAI 09.01.02-53 as shown by the gray shaded text below:

6.9 Qualification of the Bearing Pad and Bearing Pressure on the Pool Slab

Bearing pads are placed between rack pedestals and the SFP floor to reduce the compressive stresses on the SFP concrete slab by spreading the concentrated load of each pedestal over a larger contact area. This evaluation demonstrates that under maximum vertical forces in seismic events, the average compressive stress in the underlying concrete remains below the allowable value permitted by the American Concrete Institute, ACI 349-97 [6.9.1].

A bearing pad will be installed beneath all of the support pedestals on the racks in the SFP. The nominal size of the bearing pad, which is made from SA-240 304L material, is 18" × 18" × 2.5" thick.

The bearing stress in the underlying concrete is calculated by dividing the maximum pedestal load (including ACI load factors) by the contact area between the bearing pad and the SFP liner. The contact area is conservatively set equal to a 13 inch diameter circle, which means that the pedestal force spreads laterally through the bearing pad at roughly a 50 degree angle. For conservatism, the maximum calculated pedestal load from Table 6.6.1.b is used to ensure that the ultimate strength requirements from ACI 349-97 [6.9.1] are met. The calculated bearing stress is,

$$\sigma = \frac{515{,}000 lbf}{\frac{\pi}{4}(13in)^2} = 3{,}880 psi$$

The bearing pads adequately diffuse the peak pedestal load so that the compressive stress in the concrete slab is below the limit set by the governing concrete code [6.9.1] based on the design minimum concrete compressive strength of 4,000 psi. The results are summarized in the following table.

Calculated Bearing Stress on the pool slab (psi)	Allowable Bearing Stress (psi) (from Section 6.3)	Safety Factor
3,880	4,760	1.227

In addition, Holtec Report HI-2135462, Section 6.7.4, Rack Displacements and Bearing Pad Size Relative to the Displacement, will be revised to specify that spent fuel pool liner plates and fuel racks are arranged so that the maximum horizontal displacement of the fuel racks under all loading conditions, including the safe shutdown earthquake, will not result in the rack bearing plates contacting an area of the pool liner that is backed by a leak chase channel.

6.7.4 Rack Displacements and Bearing Pad Size Relative to the Displacement

The displacement results provided in Tables 6.6.2 show that maximum displacements are limited to 6.78 inch at the top and 4.72 inch at the baseplate elevation for all racks and all DYNARACK runs. To ensure there are no impacts between the racks and equipment stored in the perimeter of the spent fuel pool, there is an exclusion zone of 11 inches around the perimeter of the racks where equipment storage is prohibited. Additionally, Figure 1.1.2 shows the size and placement of each bearing pad and the positioning of the spent fuel rack pedestals on the bearing pads.

The allowable displacement limit for the pedestal supports on the spent fuel storage racks is defined as follows: the lateral displacement at the base of the rack cannot cause any portion of the adjustable male pedestal to slide off of the bearing pads at any time during the SSE event. In other words, the size and placement of the bearing pads must be such that the minimum edge distance is larger than the magnitude of the pedestal displacement. For the 7 ABWR racks, the minimum bearing pad size is specified as 18" x 18", and the outside diameter of the adjustable male pedestals is 7". Therefore, the allowable displacement limit is (18" – 7")/2 = 5.5". From Table 6.6.2, the maximum lateral displacement at the base of the spent fuel racks, from all dynamic simulations, is 4.72", which is less than the allowable limit of 5.5" indicating that the minimum bearing pad size is acceptable provided that the pedestal is centered atop the bearing pad. At locations where two or more pedestals are positioned on the same bearing pad (i.e., at rack-to-rack interfaces), the pedestals may be positioned off-center so long as the minimum distance from the pedestal to the edge of the bearing pad is greater than 5.5". Lastly, the SFP floor liner plates shall be arranged so that the maximum horizontal displacement of the fuel racks under all loading conditions, including the safe shutdown earthquake, will not result in the rack bearing pads coming in contact with an area of the pool liner that is backed by a leak chase channel.

(5) Holtec Report HI-2135462, Chapter 6, Structural/Seismic Evaluation, will be revised to reflect the size, placement and analysis of the bearing pads as described in the parts (1) through (4) above.

QUESTION:

NINA Letter, U7-C-NINA-NRC-130059, dated November 14, 2013, Attachment 5, Item 7 describes the stiffness determination of impact springs. The response referred to a publication for methodology for determining spring constants for the DYNARACK model and provided the spring values used. The staff requests that the applicant include a discussion in the report about the methodology for determining the various spring constants, including the rack-to-rack and rack-to-wall impact springs. In addition, explain what is meant by "piecewise linear friction springs."

RESPONSE:

The words "piecewise linear friction springs" refer to the bi-linear springs that are used to simulate friction behavior between the support pedestals and the bearing pads. The force-deflection shape of the "piecewise linear friction springs" is shown in the figure below:

Holtec Report HI-2135462, Section 6.4.2, Essentials of the Dynamic Model, will be revised to include a discussion about the methodology for determining the various spring constants as shown in the gray shaded text shown below:

> The previous discussion is limited to a 2-D model solely for simplicity. Actual analyses incorporate 3-D motions. The stiffness values assigned to all of the above impact springs, gap elements, etc. are provided in Table 6.4.3. The methodology used to determine the spring constants used in the DYNARACK model is provided in [6.1.2]. The rack-to-rack and rack-to-wall impact springs are determined based on the formulas given in [6.4.7] and strength of materials principles.

Holtec Report HI-2135462 will be revised to add Table 6.4.3, Stiffness Values Used in Dynamic Model, shown below in gray shaded text, which will document the stiffness values assigned to impact springs and gap elements, etc, as described above:

Table 6.4.3

STIFFNESS VALUES† USED IN DYNAMIC MODEL

Element	Stiffness Value
Rack Bending Spring (X-Z Plane), lbf-in/rad	6.572 E+10
Rack Shear Spring (X-Dir.), lbf/in	5.868 E+06
Rack Bending Spring (Y-Z Plane), lbf-in/rad	9.017 E+10
Rack Shear Spring (Y-Dir.), lbf/in	6.392 E+06
Rack Extension Spring, lbf/in	6.589 E+07
Rack Torsional Spring, lbf-in/rad	5.251 E+09
Fuel-to-Cell Impact Spring, lbf/in (Fully loaded spent fuel rack – 340 assemblies)	3.911 E+06
Pedestal Compression Spring, lbf/in	1.321 E+06
Pedestal Friction Spring, lbf/in	1.321 E+09
Rack-to-Rack Impact Spring (@ Top of Rack), lbf/in	4.310 E+05
Rack-to-Rack Impact Spring (@ Baseplate), lbf/in	4.580 E+06
Rack-to-Wall Impact Spring (@ Baseplate), lbf/in	3.860 E+06
Rack-to-Wall Impact Spring (@ Top of Rack), lbf/in	7.632 E+05

† The stiffness values given in the table are the nominal values used as input for all of the DYNARACK simulations listed in Table 6.6.1a, except for Run Nos. 17, 18, 19, 21, 22, 24, 25, 26, 28, and 29. For Run Nos. 17, 21, 22, and 24, the stiffness value of the fuel-to-cell impact springs is adjusted to reflect the number of loaded fuel assemblies in each rack. For Run Nos. 18 and 25, the stiffness values are equal to 80% of the values given in the table. For Run Nos. 19 and 26, the stiffness values are equal to 120% of the values given in the table. For Run Nos. 28 and 29, the only difference is the stiffness value for rack-to-rack impact spring at the top of rack, which are increased by 20% and 50%, respectively.

To be submitted under separate cover

QUESTION:

NINA Letter, U7-C-NINA-NRC-130059, dated November 14, 2013, Attachment 5, Item 9 discusses the energy balance method used to carry out the accidental fuel drop analysis using the Mathcad equation solver. In order for the staff to conclude that the method is acceptable, the applicant is requested to provide the following additional information:

(1) The proposed change to Holtec Report No. HI-2135462, Section 7.1.2.3, discusses the calculation of base plate deformation due to a deep drop (Scenario 1). To help the staff determine acceptability of the method, provide the derivations for the equation for baseplate deformation.

(2) The proposed change to report HI-2135462 Section 7.1.2.4 discusses the calculation of the impact force on the pedestal due to a deep drop (Scenario 2). To help the staff determine acceptability of the method, provide the derivations for the equation for the compressive stress in the pedestal.

(3) The associated mark-up of Holtec Report No. HI-2135462, Section 7, does not include Sections 7.2.1 and 7.2.2 from the original report dated July 31, 2013). Either confirm that these sections from the original report are retained, or identify where the information has been relocated.

RESPONSE:

Holtec Report HI-2135462, Chapter 7, Mechanical Accident Evaluation, will be revised to use the finite element code LS-DYNA, in lieu of the "energy balance method" for the analysis of both the shallow fuel drop and deep fuel drop scenarios. The response to RAI 09.01.02-51 provides a description of the LS-DYNA analysis and results and a markup showing changes to Holtec Report HI-2135462, Section 4.2.4.3, Assembly Dropped Vertically into a Storage Cell, and Chapter 7, Mechanical Accident Evaluation.

QUESTION:

NINA Letter, U7-C-NINA-NRC-130059, dated November 14, 2013, Attachment 5, Item 10 discusses the sliding interface between the bearing pad and the pool floor. The response states that sliding could occur either at the interface of the pedestal and the bearing pad or at the interface of the bearing pad and the pool floor liner. The response calculated the minimum available edge distance of 5.5" on the bearing pads, assuming that the pedestals are located centrally on the bearing pads. In order to complete its review, the staff needs the following clarifications:

(1) Figure 2.7, Detail F, appears to show that that the typical corner pedestals are not located centrally on the bearing pad, and may not have the minimum edge distance of 5.5". The applicant is requested to explain how minimum required edge distance is achieved for the corner pedestals including description of the bearing pads being used for adjacent rack pedestals.

(2) The response provided a mark-up of Section 6.9. It appears that the applicant updated the second paragraph of the section with the revised bearing pad size. However, the response does not include all changes needed for Section 6.9 to reflect the change to the bearing pad size. Therefore, the staff requests that the applicant revise Holtec Report No. HI-2135462, Section 6.9, to be consistent with the use of 18"x18" bearing pad size.

RESPONSE:

(1) Holtec Report HI-2135462 will be revised to include new Figure 1.1.2, Pedestal and Bearing Pad Locations for STP 3 & 4 ABWR Fuel Storage Racks. Figure 1.1.2 shows the size and position of all SFR bearing pads and the position of each pedestal on the bearing pad.

The response to RAI 09.01.02-57 includes a copy of new Figure 1.1.2, Pedestal and Bearing Pad Locations for STP 3 & 4 ABWR Fuel Storage Racks.

(2) The response to RAI 09.01.02-49, part (4), includes changes to Holtec Report HI-2135462, Section 6.9, Qualification of the Bearing Pad and Bearing Pressure on the Pool Slab, which supersede the changes described in Attachment 5, Item 10, in NINA Letter, U7-C-NINA-NRC-130059, dated November 14, 2013. These changes insure that the bearing stress in the concrete below the bearing pads is below the allowable limit.

The response to RAI 09.01.02-49, part (4), provides the changes to Holtec Report HI-2135462, Section 6.9, Qualification of the Bearing Pad and Bearing Pressure on the Pool Slab.

QUESTION:

NINA Letter, U7-C-NINA-NRC-130059, dated November 14, 2013, Attachment 5, Item 11 addresses the staff's request to perform an additional sensitivity study for analysis run number 2 with partial loading, empty rack, and reduced integration time step. The staff's review of the response to Item 11 found that two additional computer runs were performed. Run number 22 is the same as run number 17 but with COF = 0.2, instead of 0.8. Run number 23 is same as run number 2 but with a reduced time step. The staff determined that the response did not completely address the original request. It appears from the displacements listed that partial loading may increase displacements significantly. Since run number 2 has the largest displacement at the base plate level, the staff requests the applicant to conduct an analysis for run number 2 with partial loading.

RESPONSE:

Per the Staff's request, an additional WPMR run (run number 24) has been performed. Run number 24 is identical to run number 2 except that the racks are partially loaded as shown in Figure 6.6.1 of Holtec Report No. HI-2135462. The maximum displacements at the top of rack and the base plate elevation for run numbers 2 and 24 are tabulated below for comparison.

Run Number	Maximum Displacement (in)	
	Top of Rack Elevation	Base Plate Elevation
2	4.81	4.70
24	3.75	3.66

The above table shows that the maximum sliding displacement is governed by the fully loaded rack configuration (run number 2).

Also at the Staff's request, an additional WPMR run (run number 27) has been performed with a reduced time step size. The seismic response of the STP 3&4 spent fuel racks is determined by performing a series of time history simulations using the Holtec proprietary code DYNARACK. The time history simulations utilize a central difference scheme and a fixed time step to compute the response. In order to insure that the time step size is sufficiently small, a convergence study has been performed using three different time step sizes: 10×10^{-6} sec, 5×10^{-6} sec, and 2.5×10^{-6} sec. The results of the convergence study are summarized in Tables 1 and 2 below. Even when the time step size is reduced by a factor of 4, the results agree within 10 percent, which indicates that the time step size of 10×10^{-6} sec is sufficient to achieve a converged solution.

Table 1

Run No.	Time Step (x 10^{-6} sec)	Max. Stress Factor	Max. Vertical Load on Single Pedestal (lbf)	Max. Shear Load on Single Pedestal (lbf) (X or Y)	Max Fuel to Cell Wall Impact (lbf)	Max. Rack-to-Rack Impacts (lbf)	
						Top	Baseplate
11	10	0.450	487,000	252,000	1,612	-	-
20	5	0.483	458,000	276,000	1,692	-	-
27	2.5	0.477	436,000	275,000	1,697	-	-

Table 2

Run Number	Maximum Rack displacement relative to floor (inch)	
	Top of Rack	Baseplate
11	5.46	1.02
20	4.90	1.05
27	5.02	0.95

Holtec Report HI-2135462 will be revised as described in the response to RAI 09.01.02-66 to include a description and results for each of the following: the WPMR simulation for Run 24 for a partially loaded rack; the WPMR simulation for Runs 25 and 26 related to the establishment of an exclusion zone around the perimeter of the spent fuel racks as described in the responses for 09.01.02-33 and 09.01.02-66; and the WPMR simulation for Run 27 which used reduced time step size as described above.

QUESTION:

In NINA letter, U7-C-NINA-NRC-130059, dated November 14, 2013, Attachment 5, Item 16, the applicant provided additional information on gaps between racks, between fuel and cell wall, and between rack and pool wall. The response states:

> HI-2135462 addresses each of these issues as follows: [...]
> e) Following a seismic event, confirmation of the rack to rack gaps will be necessary to ensure the post-seismic rack configuration is acceptable. If the gaps are outside of tolerance limits, then the racks must be re-positioned or a reconciliation analysis must be performed.

The staff is unable to locate this information in the report; therefore, the staff requests that the applicant identify where this requirement is located in the report; otherwise, add the requirement to the report.

RESPONSE:

Requirements for post-earthquake actions are not specified in Holtec Report HI-2135462. NINA believes the appropriate location for this information is in the FSAR with other requirements associated with post-earthquake actions.

COLA Part 2, Tier 2, Section 3.7.5.2, Pre-Earthquake Planning and Post-Earthquake Actions, specifies requirements for procedures for post-earthquake actions. To ensure that post-earthquake actions specifically address potential concerns with the spent fuel racks, NINA will revise FSAR 3.7.5.2 as shown in the highlighted text below:

3.7.5.2 Pre-Earthquake Planning and Post-Earthquake Actions

The following standard supplement addresses COL License Information Item 3.20.

The procedures for pre-earthquake planning and post-earthquake actions will be developed in accordance with Subsection 3.7.4 and Section 13.5 prior to fuel load. The procedures will implement the seismic instrumentation program specified in Subsection 3.7.4 and follow the guidelines recommended in EPRI Report NP-6695 (Reference 3.7-7), with the exceptions listed in Subsection 3.7.5.2 of the reference DCD. (COM 3.7-1)

In addition, the procedures address measurement of the post-seismic event gaps between the spent fuel racks and between the spent fuel racks and the spent fuel pool walls and require appropriate corrective actions (such as repositioning the racks or analysis of the as-found condition) if needed.

QUESTION:

NINA Letter, U7-C-NINA-NRC-130059, dated November 14, 2013, Attachment 5, Item 18 discusses whether all fuel racks are permanently installed in the spent fuel pool. The response states:

> HI-2135462, which is incorporated by reference into the STP 3 & 4 FSAR, requires that all seven spent fuel racks are installed in the spent fuel pool. Any alternate layout will require approval in accordance with the regulatory change processes from 10 CFR Part 52 or Part 50, as appropriate.

The staff is unable to locate this information in the report; therefore, the staff requests that the applicant identify where the statements are located in the report; otherwise, add the statements in the report.

RESPONSE:

NRC regulations require that each nuclear facility be maintained as described in the final safety analysis report (FSAR) (as updated) in accordance with 10 CFR 50.59. 10 CFR 50.59 requirements apply to both the design and the supporting analysis.

The STP 3 & 4 FSAR provides the description of the spent fuel racks and the supporting analyses by direct reference to "Holtec International Licensing Report for South Texas Project UNITS 3 & 4 ABWR Spent Fuel Racks" (HI-2135462)" in FSAR Sections 9.1.6.3, Spent Fuel Storage Racks Criticality Analysis, 9.1.6.4, Spent Fuel Racks Load Drop Analysis, and 9.1.6.7, Spent Fuel Racks Structural Evaluation. Therefore, any changes to the spent fuel racks that affect either the design or supporting analyses of the racks as described in HI-2135462 must be evaluated in accordance with 10 CFR 50.59 as a change to the FSAR.

Holtec Report HI-2135462 describes the design of the spent fuel racks as consisting of seven (7) storage racks and describes the supporting analyses as being performed on all seven (7) storage racks configured as described in HI-2135462. The references in HI-2135462 that describe seven spent fuel racks include:

> Section 1.1, Introduction, which specifies "This pool contains seven (7) ABWR storage racks which are designed to handle irradiated and/or non-irradiated fuel assemblies (i.e. do not rely on fuel burnup for reactivity compliance)."
>
> Section 2.1, Introduction, which specifies "The Spent Fuel Pool (SFP) will be equipped with seven 17 x 20 non-safety related, Seismic Category I, fuel storage racks with a total storage capacity of 2380 ABWR fuel assemblies."
>
> Section 6.6, Dynamic Simulations, which specifies "As shown in Figure 1.1.1, the layout will contain seven (7) ABWR racks."

Based on the above, storage of new or spent fuel in the spent fuel rack with less than seven (7) racks in the spent fuel pool would constitute a change to the design and the supporting analysis as described in the FSAR and would have to be evaluated and approved in accordance with requirements in 10 CFR 50.59.

QUESTION:

NINA Letter, U7-C-NINA-NRC-130059, dated November 14, 2013, Attachment 5, Item 21 discusses the number and locations of support feet for the spent fuel racks. The staff determined that there is no figure in Holtec Report No. HI-2135462 showing a plan view, with dimensions, of the locations of all support feet and bearing pads for the 7-rack configuration. Therefore, the staff requests that the applicant provide a figure in Holtec Report No. HI-2135462 of a plan view showing the locations of the support feet and bearing pads for all the racks in the spent fuel pool, with dimensions.

RESPONSE:

The information requested will be added to Holtec Report HI-2135462, as Figure 1.1.2, Pedestal and Bearing Pad Locations for STP 3 & 4 ABWR Fuel Storage Racks, a copy of which is provided with this response.

Holtec Report HI-2135462 will be revised as shown in the following highlighted text:

1.1 Introduction

The spent fuel pool is inside the plant's Reactor Building. The SFP is a reinforced-concrete fuel storage pool with a stainless-steel liner. This pool contains seven (7) ABWR storage racks which are designed to handle irradiated and/or non-irradiated fuel assemblies (i.e. do not rely on fuel burnup for reactivity compliance). Figure 1.1.1 and Figure 1.1.2 shows the layout of the SFP storage racks.

Additionally, HI-2135462, Section 6.7.4, Rack Displacements and Bearing Pad Size Relative to the Displacement, will be revised to include the following:

Figure 1.1.2 shows the size and placement of each bearing pad and the positioning of the spent fuel rack pedestals on the bearing pads.

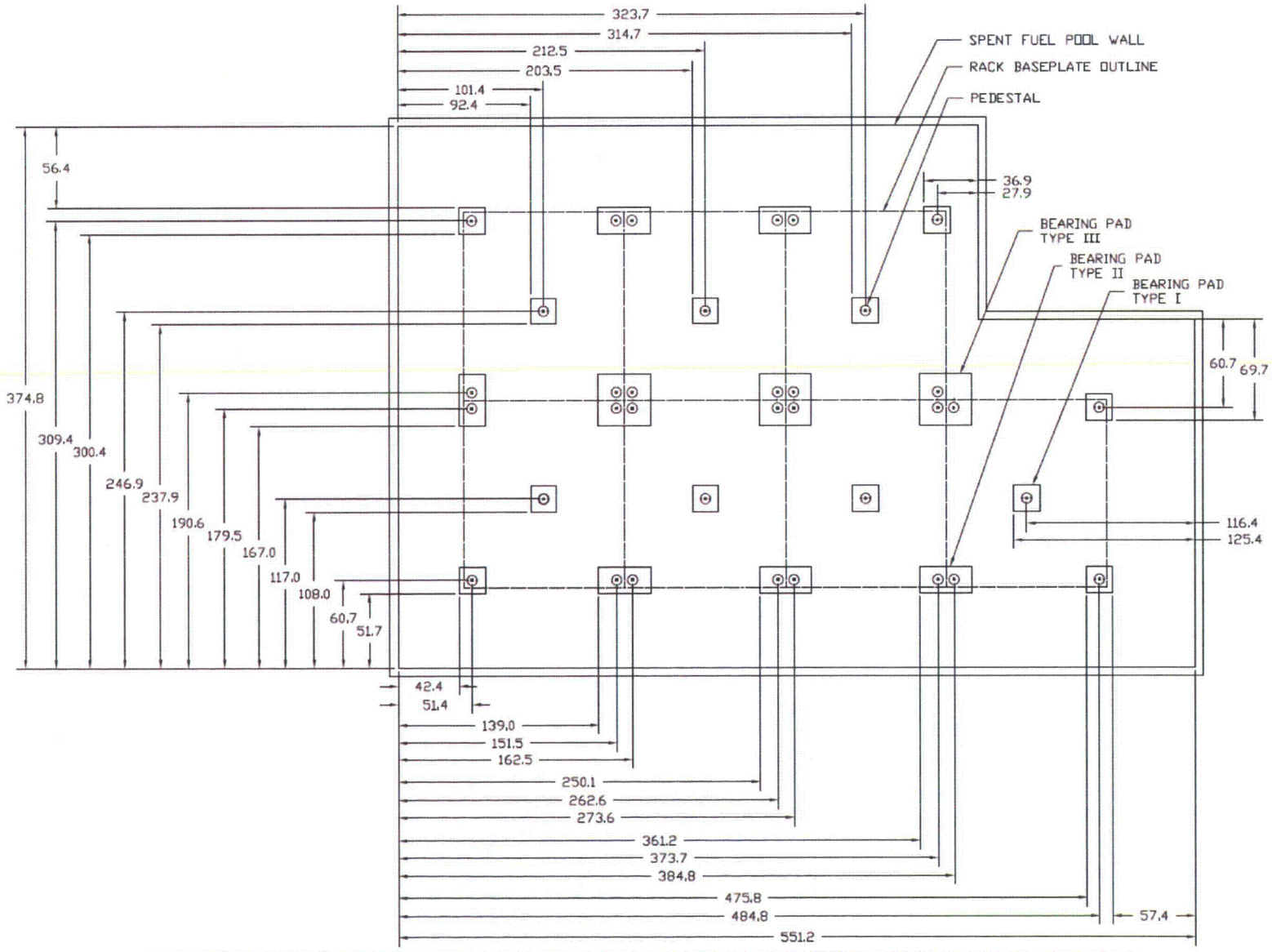

Figure 1.1.2 – Pedestal and Bearing Pad Locations for STP 3 & 4 ABWR Fuel Storage Racks
(All dimensions are nominal)

QUESTION:

NINA Letter, U7-C-NINA-NRC-130059, dated November 14, 2013, Attachment 5, Item 25 discusses the thermal loads. The response provided information on the thermal conditions considered in the analysis and design of the fuel racks. The staff's review of Holtec Report No. HI-2135462 found that the report did not explain why the thermal load at the base of a pedestal, due to expansion of the rack, is not considered. The applicant is requested to address this issue by considering that friction at the base of a pedestal will likely induce lateral force at the base of the pedestal.

RESPONSE:

The spent fuel racks are freestanding. As a result, during a design basis seismic event the racks will rock causing momentary lift off of the rack pedestals from the bearing pads. This behavior is confirmed by the results of the Whole Pool Mulit-Rack (WPMR) dynamic simulations. The first time that a pedestal lifts off from a bearing pad, any lateral force on the pedestal due to restraint of thermal expansion is reduced to zero.

Under normal conditions, the lateral force at the base of the pedestal is limited by the pedestal's friction capacity. From Section 6.7.3.1 of Holtec Report No. HI-2135462, the maximum dead load on a single pedestal under normal conditions is 54,500 lbf. Based on an upper bound coefficient of friction of 0.8, the pedestal's friction capacity is 0.8 x 54,500 lbf = 43,600 lbf. On the other hand, the maximum shear load on a single pedestal under SSE conditions is 321,000 lbf. Since the normal (Service Level A) load is less than 15% of the accident (Service Level D) load, while the Level A limits equal or exceed 50% of the Level D limits, the SSE load condition bounds the dead load condition and no further evaluation of the lateral force at the base of the pedestal due to restraint of thermal expansion is needed.

QUESTION:

NINA Letter, U7-C-NINA-NRC-130059, dated November 14, 2013, Attachment 5, Item 36 discusses the modeling of fluid coupling. The response described the methodology for modeling fluid around the rack. The staff requests that the applicant update the report to include the information provided in the response.

RESPONSE:

Holtec Report HI-2135462, Section 6.4, Dynamic Analysis Methodology, will be revised to include the following highlighted text just before the final paragraph of that section:

With regard to the water above and below the racks, the hydrodynamic coupling between the rack baseplate and the spent fuel pool liner is captured in the DYNARACK simulation model, while the water above the racks is not. The latter is not included for the following reason. The spent fuel racks are situated at the bottom of the Spent Fuel Pool greater than 20 feet below the surface of the water, which is outside of the influence of the convective (sloshing) water mass. Therefore, the water above the racks has no effect on the seismic response of the spent fuel racks.

Rack-to-rack and rack-to-wall fluid coupling are determined using DYNARACK simulations. The spent fuel racks in a Spent Fuel Pool are represented by an array of rectangles in the DYNARACK model, which are surrounded by narrow fluid filled channels. The spent fuel pool walls enclose the entire array of racks. Fluid flow in the channels is evaluated with classical fluid mechanics principles. Each rectangular body (fuel rack) has horizontal velocity components and the pool walls are also assumed to move.

During a seismic event, the pool walls and the spent fuel racks are subject to inertia forces that induce motion to the rectangular racks and to the walls. This motion causes the channel widths to change and causes flow to occur in each of the channels. Because all of the channels are connected, the equations of classical fluid mechanics can be used to establish the fluid velocity (hence, the fluid kinetic energy) in terms of the motion of the spent fuel racks.

Once the velocities are determined in terms of the rack motion, the kinetic energy can be written and the fluid mass matrix identified. The fluid mass matrix can then be solved as a function of height in each of the two horizontal directions.

The approach used for fluid coupling between the fuel assemblies and the cell walls is based on Fritz's classical two-body fluid coupling model [6.1.2, 6.4.6].

The structural mass effects and the hydrodynamic effect from fluid within the narrow annulus in each cell between the fuel assembly and the cell wall is incorporated in the DYNARACK model.

QUESTION:

NINA Letter, U7-C-NINA-NRC-130059, dated November 14, 2013, Attachment 5, Item 38 discusses stiffness and damping of fuel assemblies. The response states that the fuel assemblies are modeled as uncoupled lumped masses, and that there is no structural damping associated with the modeling of the fuel assemblies. The response refers to a publication for determining the spring stiffness for fuel to cell wall impact. However, it is not clear to the staff if modeling of the fuel assembly as uncoupled masses, which does not take into account the elastic properties of the fuel assembly and the lateral support at the base plate, will result in a conservative estimate of impact loads on the fuel assembly. The staff requests that the applicant provide the technical basis for this assumption. Additionally, the response indicates that impact spring stiffness for the fuel assembly lumped masses is calculated assuming impact is simulated by a uniform pressure on a circular section of cell wall with a radius larger than half of the inside dimension of the cell. Provide the technical basis for this approach.

RESPONSE:

The underlying rationale for the modeling features such as the computation of the contact stiffness between the fuel and the rack's cell wall and depiction of fuel assemblies as lumped mass elements noted by the Staff lies in the specific mission of the rack's dynamic model. The objective of the dynamic model is to serve as the vehicle for the safety analysis of the *freestanding racks* under seismic loadings. For freestanding racks, a principal focus of the safety analysis is to quantify their kinematic motion (rocking, sliding, precession, etc.) including the potential for inter-rack impacts (which may cause severe plastic deformation of the cell openings preventing future retrievability of fuel).

As to the racks themselves, there are two discrete regions with different structural attributes, namely the cellular region (above the baseplate) and the support pedestals (below the baseplate). Of the two, the support pedestals are evidently most stressed because they must withstand the cumulative inertia loads from the rattling fuel assemblies in the cellular region above and the friction forces at their base (transmitted from the pool's support surface). The cellular region made up of a honeycomb arrangement of inter-connected cells has a large section modulus which ensures that the cross sectional shear and bending stresses in it (required of Section III Class 3 linear structures) are quite small. The support pedestals, possessed of a much smaller section moduli, on the other hand, are apt to be highly stressed.

Guided by the above insights, the dynamic model of the rack module (shown in Figures 6.4.1 through 6.4.5 of Holtec Report No. HI-2135462) represents each pedestal explicitly as a "beam element" but lumps the cumulative stiffness of the cellular region as a set of single beam elements in series. Within the framework of this simplified model, it was necessary to simulate the mass of the fuel assemblies and their internal rattling effect in a manner that maximizes the kinematic response of the rack. For this purpose, all of the fuel assemblies in the rack are lumped into the physical space occupied by one assembly thus postulating that they will all vibrate in *unison.*

The mass distribution of this aggregated fuel assembly is represented by up to five lumped masses (some licensing submittals have used as few as two) arrayed at uniform vertical intervals. The impulse of the impact between the fuel and the cell wall is maximized by assuming the fuel lumped mass to be rigid (in reality, a fuel assembly's lateral surface is flexible to various degrees depending on the fuel type). The stiffness of the impacted surfaces (cell wall) is likewise over-estimated by assuming that it is defined by a circular plate of the cell wall's thickness fixed at its periphery. The stiffness of each impacted surface is equal to that of one plate times the number of fuel assemblies. In this manner, the impulse of rattling impact is maximized. A paper, published in Nuclear Engineering & Design entitled "Seismic Response of a Free Standing Fuel Rack Construction to 3-D Floor Motion" which was included as Attachment 3 to Letter U7-C-NINA-NRC-130059, dated November 14, 2013 (ML13326A573), contains additional modeling details and may be consulted for further information in this matter.

In earlier licensing submittals (in the 1980s), the super-masses representing the fuel assemblies were connected by bending and shear springs derived from the beam bending characteristics of the stored assemblies. Analyses of fuel racks of this model, however, showed that the fuel assembly springs were so overshadowed by the those representing the cellular region that it was immaterial whether they were included or not.

In order to demonstrate that the 5 lumped mass model employed by the computer code DYNARACK conservatively predicts the maximum fuel-to-cell impact loads, a series of DYNARACK simulations have been performed in which the stiffness properties of the stored fuel have been varied from infinitely flexible (i.e., zero bending stiffness) to essentially rigid. The results show that when the stored fuel assemblies are considered as infinitely flexible the maximum fuel-to-cell impact load is conservatively overestimated as compared to the solution corresponding to the calculated fuel assembly stiffness.

In the standard DYNARACK model, the stored fuel assemblies in each individual rack are modeled as a set of five lumped masses equally spaced over the height of the storage cells at elevations 0, 0.25H, 0.5H, 0.75H, and H (where H is the height of the storage cells above the rack base plate). The DYNARACK model conservatively assumes that all of the stored fuel assemblies move in phase, and therefore each of the five lumped masses represents the totality of the stored fuel mass at that elevation. In other words, the three intermediate lumped masses (i.e., nodes 3*, 4*, and 5* in Figure 6.4.1 of HI-2135462) are each assigned 25% of the total stored fuel mass, and the top and bottom lumped masses (i.e., nodes 1* and 2* in Figure 6.4.1 of HI-2135462) are each assigned 12.5% of the total stored fuel mass. Thus, the sum of the five lumped masses equals 100% of the total stored fuel mass.

Fluid coupling effects between the stored fuel assemblies and the storage cell walls are accounted for in the DYNARACK model. The magnitude of the fluid coupling forces, however, is conservatively computed based on the mean fuel-to-cell wall gap at time zero. That is to say the fluid coupling forces are not re-computed at each time step based on the current position of the lumped fuel masses. This is conservative because the fluid coupling forces are inversely proportional to the gap size. Thus, the fluid coupling force would increase as the lumped fuel mass approaches the cell wall, which would attenuate the fuel-to-cell impact load. In addition,

the DYNARACK solution neglects fluid damping and form drag associated with the motion of the fuel assemblies.

Each lumped fuel mass in the DYNARACK model has two horizontal degrees of freedom (DOF) in the x and y directions, as shown in Figure 6.4.1 of Holtec Report No. HI-2135462. In the standard DYNARACK model, the five lumped masses move independently from each other in the x and y directions as if the stored fuel assemblies have zero lateral stiffness. To study the effects of fuel assembly stiffness, the standard DYNARACK model has been modified to introduce two linear springs (one each in x and y directions) between each pair of adjacent fuel masses (e.g., nodes 2* and 3* in Figure 6.4.1). Consequently, there are a total of 8 springs (4 node pairs x 2 directions) connecting the 5 fuel masses (per rack) in the modified DYNARACK model. This means that 56 additional springs (8 springs per rack x 7 racks) are added to the overall model. There are no changes to the fuel-to-cell impact springs, which are described in Section 6.4.2 and depicted in Figure 6.4.2. Although adding these springs is intended to represent a "more realistic" fuel assembly, only limited credit is taken for fuel assembly damping. Fuel assembly damping as high as 10% could be credited based on available data, but the DYNARACK model only credits 4% damping.

Using the modified model, twelve 12 DYNARACK simulations have been performed in which the stiffness value assigned to the 56 fuel springs ranges from a minimum of 10 lbf/in to a maximum of 10^7 lbf/in. Apart from the fuel springs, these 12 runs are otherwise identical to Run No. 19 from Holtec Report No. HI-2135462, which produced the maximum fuel-to-cell impact load of 1,774 lbf. (Note: Although there are no fuel springs associated with Run No. 19, it is shown in the table below as having a spring stiffness of 0.1 lbf/in solely for the purpose of estimating a fuel assembly response frequency.) The fuel-to-cell impact results from these 12 runs (plus Run No. 19 from HI-2135462) are summarized in the table below. The maximum fuel-to-cell impact loads are also plotted versus the fuel assembly spring stiffness at the end of this paper.

Spring Stiffness (lbf/in)	Frequency (Hz)	Top/Bottom Fuel-to-Cell Impact (lbf)	Intermediate Fuel-to-Cell Impact (lbf)
0.1 (Run No. 19)	0.003	1,018	1,774
10	0.032	1,004	1,791
50	0.071	1,012	1,776
100	0.100	1,023	1,788
500	0.223	1,013	1,776
1,000	0.316	1,019	1,773
10,000	0.999	1,020	1,708
100,000	3.160	1,009	1,576
340,000 (Calculated Estimate)	5.827	1,251	1,452
500,000	7.066	1,426	1,476
1,000,000	9.992	1,566	1,867
5,000,000	22.344	1,405	1,423
10,000,000	31.599	1,389	1,555

In the above table, the spring stiffness of 340,000 lbf/in is identified as the "calculated estimate" meaning that it has been calculated based on the geometry and material properties of the fuel assembly as opposed to an arbitrarily chosen value. To calculate the stiffness of the ABWR fuel assembly, the channeled fuel assembly is treated as a simply supported beam subjected to a concentrated load P at its midspan, as shown in the following sketch (where L is the length of the fuel assembly).

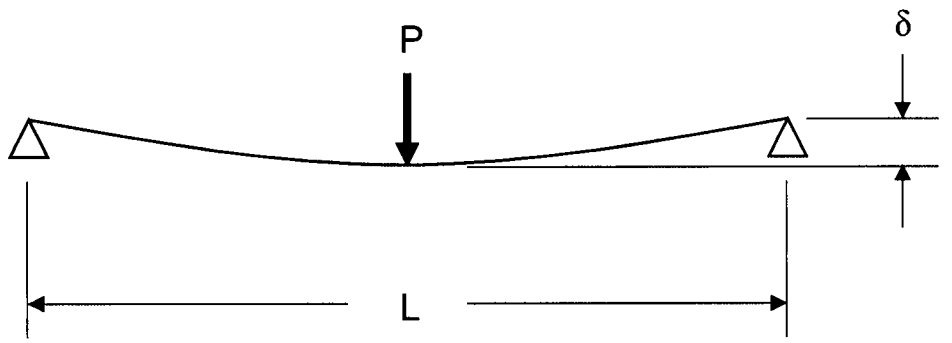

The stiffness is then computed as the concentrated load (P) divided by the maximum deflection (δ) at the center of the beam (i.e., K = P / δ). The five lumped mass model yields the same deflection (δ) when the model is subjected to the same loading (i.e., the top and bottom nodes are restrained and a concentrated load P is applied to the center node) and the stiffness of the fuel springs is set equal to K. For the design basis ABWR fuel assembly, the calculated stiffness is roughly 1,000 lbf/in. The fuel assembly internals (i.e., fuel rods) do not contribute significantly to the overall stiffness of the fuel assembly. This is confirmed by the numerical studies performed by PNNL[1] in which a detailed finite element model of an unchanneled BWR fuel assembly is subjected to a concentrated force of 30 kgf near its midspan. The maximum calculated lateral deflection of the fuel assembly is 27.2 mm, which indicates that the equivalent stiffness of fuel assembly internals is only 61.7 lbf/in (= 30 kgf / 27.2 mm) or roughly 6 percent of the stiffness of the BWR channel.

Therefore, for a fully loaded rack containing 340 ABWR fuel assemblies, the total effective stiffness for input to the DYNARACK model is 340 fuel assemblies x 1,000 lbf/in per assembly = 340,000 lbf/in.

To verify the calculated stiffness used as input to DYNARACK, the first mode frequency of the five lumped mass model (with its end nodes restrained) is compared to the natural frequency of an ABWR fuel assembly when it is treated as a simply supported beam. The results compare quite favorably. The frequency of the five lumped mass model is 5.827 Hz as compared to a frequency of 5.438 Hz for the simply supported beam. These results also compare favorably to

[1] N. Klymyshyn et al., "Fuel Assembly Shaker Test Simulation", Pacific Northwest National Laboratory, May 30, 2013.

physical test measurements of a BWR fuel assembly, which yielded a natural frequency of approximately 4.8 Hz[2].

After reviewing the results of the study, the following observations can be made:

1) The maximum fuel-to-cell impact loads are essentially unchanged for spring stiffness values ranging between 0.1 lbf/in and 1,000 lbf/in.
2) Above 1,000 lbf/in, the maximum fuel-to-cell impact loads at the intermediate node locations trend downward until K = 340,000 lbf/in.
3) Between K = 340,000 lbf/in and K = 5,000,000 lbf/in, the fuel-to-cell impact loads increase to a maximum of 1,867 lbf due to resonance.

The resonance effect that is observed when K = 1,000,000 lbf/in is not a credible concern because it requires a fuel assembly stiffness that is roughly three times greater than the calculated stiffness value. More importantly when K = 340,000 lbf/in (which corresponds to the calculated fuel assembly stiffness) the maximum fuel-to-cell impact load is only 1,452 lbf, which is significantly less than the maximum impact load reported in Holtec Report HI-2135462 for Run No. 19 (1,774 lbf). However, the maximum impact load at a top/bottom node location is 1,251 lbf, which is greater than the value (1,018 lbf) for Run No. 19. For conservatism, this higher impact load at the fuel assembly top/bottom has been considered as input to the structural evaluation of the stored fuel assembly (see RAI 09.01.02-45).

[2] H. Sato et. al., "Test Results on Seismic Proving Test of BWR Core Internals".

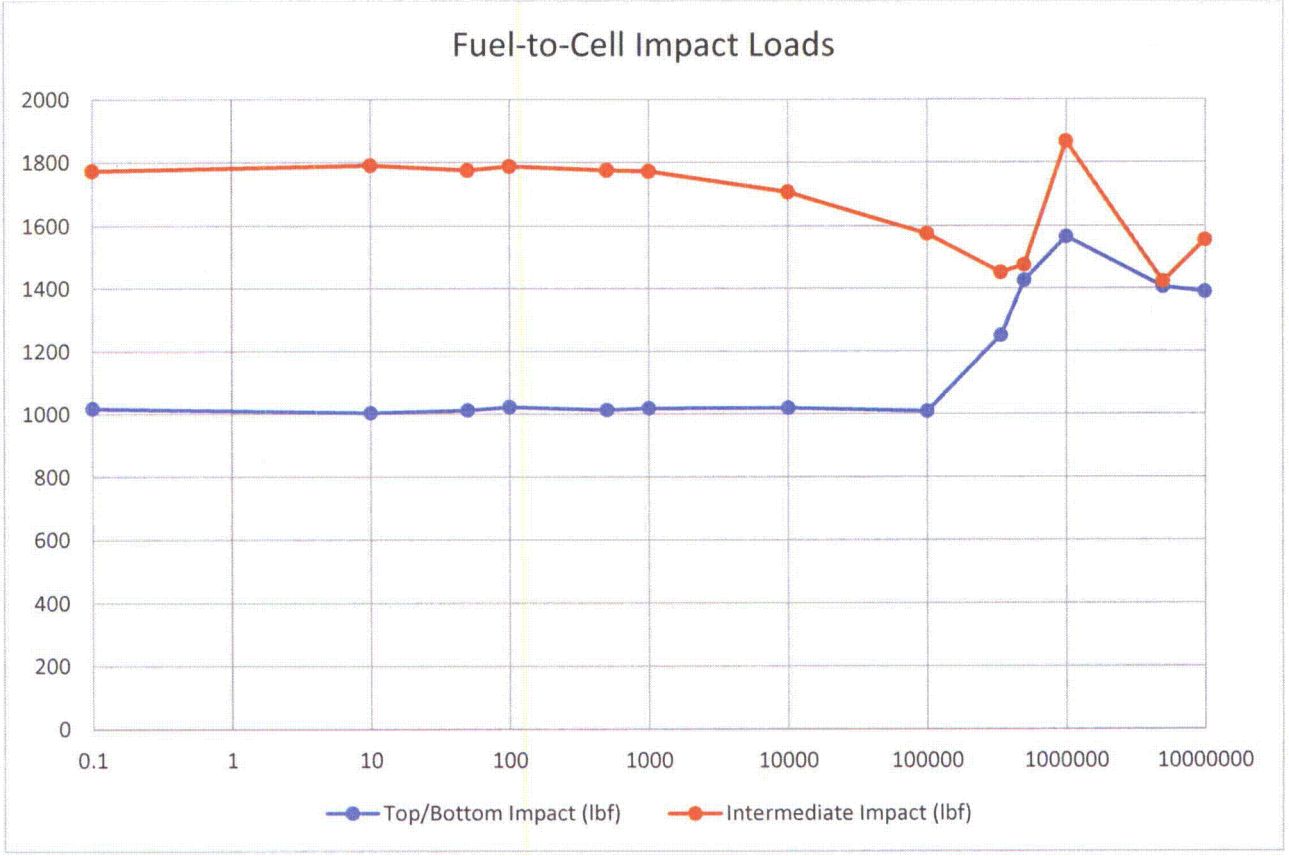

Based on the response above, part b of HI-2135462, Section 6.4.2, Essentials of the Dynamic Model, will be revised as shown in gray shaded text below.

b. Rattling fuel assemblies within the rack are modeled by five lumped masses located at H, 0.75H, 0.5H, 0.25H, and at the rack base (H is the rack height measured above the baseplate). Each lumped fuel mass has two horizontal degrees-of-freedom, and its horizontal motion is independent from the other fuel masses. In other words, the five fuel masses are decoupled from one another in the horizontal direction. Vertical motion of the fuel assembly mass is coupled to rack vertical motion at the baseplate level. The centroid of each fuel assembly mass can be located off-center, relative to the rack structure centroid at that level, to simulate a partially loaded rack.

It is highly unlikely, if not impossible, that two adjacent fuel assemblies move 180° out of phase towards each other such that they impact the cell wall at precisely the same instant in time at the same vertical location. Fuel assemblies are much more likely to rattle in unison, like multiple clappers in a bell. A Japanese study constructed a full-scale free-standing spent fuel rack loaded with

fuel assembly masses. The full scale model was tested on a shaker table to record the seismic response of the rack and fuel assemblies. The test results clearly show that the fuel assemblies rattle in unison, thereby justifying the accepted analytical practice of modeling all the fuel assemblies in a rack as a single large segmented mass [6.4.8].

In order to demonstrate that the 5 lumped mass model employed by the computer code DYNARACK conservatively predicts the maximum fuel-to-cell impact loads, a series of test simulations have been performed in which the stiffness properties of the stored fuel have been varied from infinitely flexible (i.e., zero bending stiffness) to essentially rigid. The results show that when the stored fuel assemblies are considered as infinitely flexible the maximum fuel-to-cell impact load is conservatively overestimated as compared to the solution corresponding to the calculated fuel assembly stiffness, except at the top/bottom fuel nodes (i.e., node locations 1* and 2* in Figure 6.4.1) [6.7.10]. The higher impact load at the top/bottom fuel nodes is evaluated further in Section 6.7.1.1.

QUESTION:

NINA Letter, U7-C-NINA-NRC-130059, dated November 14, 2013, Attachment 5, Item 43 discusses the modeling of weld details. The response states that the forces acting on the cell to baseplate welds are determined with the aid of ANSYS; however, Section 6.7.9 of the Holtec Report No. HI-2135462 does not mention use of ANSYS for cell to base plate welds. The staff requests that the applicant explain the inconsistency.

RESPONSE:

NINA Letter, U7-C-NINA-NRC-130059, dated November 14, 2013, Attachment 5, Item 43 contains a typographical error. The response should state: "The weld strength evaluations are performed using the classical weld analysis method, except that forces acting on the pedestal-to-baseplate weld are determined with the aid of the finite element code ANSYS."

Holtec Report HI-2135462, Section 6.7.9, Weld Stresses, Part b, Baseplate-to-Pedestal Welds, summarizes the analysis of the baseplate-to-pedestal welds using the finite element code ANSYS. The analysis of this weld assumes that the compression load on the pedestal is resisted by metal to metal contact between the top of the pedestal and the baseplate, and therefore the baseplate-to-pedestal weld resists only the horizontal shear load on the pedestal and the net tension on the weld due to bending.

Holtec Drawing 8946 has been revised to include a note that requires the female pedestals to be clamped in place prior to welding to maximize contact with baseplate. In addition, the top surface of the female pedestals is specified as a machined surface to insure it is smooth and flat and that there is no gap between the pedestal and the baseplate after welding.

Finally, Holtec Report HI-2135462, Section 2.6, Rack Fabrication, will be revised to include the gray shaded text shown below:

> In the final step, adjustable support pedestals (shown in Figure 2.5) are welded to the underside of the baseplate maintaining metal to metal contact between the top of the pedestal and the baseplate.

QUESTION:

NINA Letter, U7-C-NINA-NRC-130059, dated November 14, 2013, Attachment 5, Item 46 discusses the validation of computer codes. The staff review of Holtec Report No. HI-2135462 did not find sufficient information on this issue. The staff requests that the applicant include a list of all computer codes used, including a description of scope of use and validation information for their use.

RESPONSE:

Holtec Report HI-2135462 will be revised to add new Section 6.4.4, Computer Codes, to list computer codes used, a description of how the code was used in the analysis, and a description of the validation. Holtec Report HI-2135462, Section 6.4.4, Computer Codes, is shown as gray shade text below:

6.4.4 Computer Codes

The following computer codes have been used to perform the seismic/structural analysis of the spent fuel racks:

EZ-FRISK is used to develop modified real recorded acceleration time histories from design basis floor response spectra to be used in non-linear time history analysis. The validation report, HI-2135536 [6.4.10], which has been prepared in compliance with SRP 3.8.1, Subsection II.4.F, addresses use of the program to develop modified real recorded acceleration time histories from design basis floor response spectra.

The Holtec proprietary computer code DYNAMO (which is also referred to herein and in previous licensing applications by its legacy name DYNARACK) is used to perform 3-D non-linear time history analysis of freestanding spent fuel racks under earthquake loading. The validation reports, HI-91700 and HI-2114848 [6.4.3], have been prepared in compliance with SRP 3.8.1, Subsection II.4.F. HI-91700 has been submitted to the NRC under previous licensing applications (Docket No. 50-382). As a further validation of the DYNAMO code, a benchmark comparison was previously performed between a 22 degree of freedom DYNAMO model and a detailed 3-D finite element model created using LS-DYNA. The two single rack models were constructed for the same rack geometry and were subjected to identical seismic inputs. It was found that the DYNAMO model produced larger rack displacements and fuel impact loads as compared to the LS-DYNA solution, thus indicating that the DYNAMO solution was more conservative. This benchmark study, along with its findings, was presented to the NRC in a previous RAI response [6.4.9] from a prior licensing application.

ANSYS is used to model the stresses in the pedestal-to-baseplate weld and to evaluate the potential for cell wall buckling. The validation report, HI-2012627 [6.4.11], has been prepared in compliance with SRP 3.8.1, Subsection II.4.F.

LS-DYNA is used to evaluate the capacity of the rack bumper bars to withstand rack-to-rack impact loads and to analyze the fuel drop accidents in Chapter 7. The validation report, HI-961519 [6.4.12], has been prepared in compliance with SRP 3.8.1, Subsection II.4.F.

Mathcad, Version 15, was used to perform miscellaneous stress calculations for the spent fuel racks. Mathcad satisfies validation requirements described in SRP 3.8.1, Subsection II.4.F, in that the computer program is commercially available and widely used and has had sufficient history of use to justify its applicability and validity without further demonstration.

The following references will also be added in Section 6.12 of Holtec Report HI-2135462:

[6.4.9] FENOC Letter L-10-151, "Response to Request for Additional Information for License Amendment Request No. 08-027 (TAC No. ME1079)," dated May 21, 2010 (ML101460057).

[6.4.10] Holtec Report HI-2135536, "Validation of EZ-FRISK Computer Code", Rev. 1.

[6.4.11] Holtec Report HI-2012627, "QA Documentation Package for ANSYS (Versions 11.0 and higher)", Rev. 10.

[6.4.12] Holtec Report HI-961519, "LS-DYNA QA Validation", Rev. 11.

QUESTION:

In NINA letter, U7-C-NINA-NRC-130059, dated November 14, 2013, Attachment 5, the response to Item 48 provided the seismic analysis results of maximum rocking and uplift of the fuel racks. The applicant is requested to include in Holtec Report No. HI-2135462 the evaluation results of maximum rocking angle of the rack and the maximum uplift height of a support pedestal.

RESPONSE:

Section 6.7.2 of the Holtec licensing report, HI-2135462, will be updated with the following:

6.7.2 Kinematic Stability Determination

The maximum rocking angle of a rack is determined based on the maximum top of rack displacement (6.78") from Table 6.6.2 and the overall height of a rack above the bearing pad (179.25"). Assuming that the top of rack displacement is caused entirely by rocking (i.e., no sliding), the maximum rocking angle of a rack is 2.17 degrees. The critical rocking angle, which would cause the rack to overturn, is 29.2 degrees. Therefore, the racks have a large margin of safety against overturning due to a seismic event. Based on a maximum rocking angle of 2.17 degrees, the maximum uplift height of a support pedestal is 3.8 inches.

QUESTION:

NINA Letter, U7-C-NINA-NRC-130059, dated November 14, 2013, Attachment 5, Item 50 discusses details of the methodology used to calculate buckling stress in the cell wall at the bottom of the rack. The response states:

> The modeled height of the cells is 4.875", which equals the distance from the top of the rack base plate to the bottom of the neutron absorber sheathing. This is the most critical area for buckling since the cell wall acts alone in compression. Above 4.875" the buckling potential is diminished due to the presence of the neutron absorber sheathing, which is welded directly to the cell wall.

The staff's review of the response found that additional justifications are needed for the approach used. The applicant is requested to provide the following additional information:

(1) The response states that the top edges of the finite element model are laterally restrained in the x and y directions. Provide the technical basis for the boundary constraint assumed in the design-basis buckling evaluation, including results of any sensitivity study due to variations in the boundary constraints.

(2) The staff notes that the integrity of the welds connecting the sheathing to the cell wall appears to be assumed. Provide the technical basis for this assumption including details of evaluation of the sheathing-to-cell wall attachment welds.

(3) It is not clear from the response to Item 50 whether the maximum predicted cell wall compressive stress at any location in any rack is used in the buckling evaluation. Provide a figure of the 7-rack arrangement showing the horizontal and vertical location of maximum compressive stress in the cell wall. Define the magnitude of compressive stress and confirm that this value is used in the buckling evaluation. If this is not the case, explain why a lower value is appropriate.

RESPONSE:

(1) The top edges of the 3 x 3 cell model are laterally restrained in the x and y directions to effectuate simply supported boundary conditions for all cell walls. This allows the top edge of each cell wall to rotate freely about its edge axis under the applied compression load. In reality, the continuation of the cell wall above the height of 4.875" provides some resistance against rotation and enhances the cell wall buckling capacity as compared to the finite element model. his analysis method, including the boundary conditions, has been reviewed and accepted by the NRC for a previous spent fuel rack licensing application.

Nonetheless, to insure that the solution is conservative, the cell length has been increased from 4.875" (per the original analysis) to 10" in the FE model, and the analysis has been

re-performed. Based on Timoshenko and Gere's Theory of Elastic Stability (2nd Edition), the 10" length is sufficient to eliminate the effects from the imposed boundary conditions at the top edges of the FE model. This is because, per Article 9.5 of cited reference, the critical buckling force for a rectangular plate simply supported along two opposite sides (and uniformly compressed in the direction parallel to those sides) is relatively constant for plates having a length to width ratio above 1.316. For the STP 3&4 spent fuel racks, the cell width (or cell inner dimension) is equal to 6.0". Therefore, the critical buckling load will not vary significantly for cell lengths greater than 1.316 x 6.0" = 7.896". For this reason, a cell length of 10" has been chosen for the FE model.

Based on the above information, the text in Section 6.7.10, Potential for Cell Wall Buckling, of Holtec Report No. HI-2135462 will be revised as follows:

The finite element model, which is shown in Figure 6.7.1, represents a 3 x 3 array of storage cells at a rack corner location. The modeled height of the cells is 10", which exceeds the distance from the top of the rack base plate to the bottom of the neutron absorber sheathing. No credit, however, is taken for the stiffening effect of the neutron absorber sheathing, which is welded directly to the cell wall. This is the most critical area for buckling since the compressive stresses are maximum at the base of the cells. The bottom edges of the finite element model are simply supported, and the top edges are laterally restrained in the x and y directions. The cell walls are assigned bi-linear elastic plastic material properties consistent with the strength properties of SA-240 304 at 200°F.

Based on Timoshenko and Gere's Theory of Elastic Stability [6.7.9], the 10" cell length is sufficient to eliminate the effects from the imposed boundary conditions at the top edges of the FE model. This is because, per Article 9.5 of [6.7.9], the critical buckling force for a rectangular plate simply supported along two opposite sides (and uniformly compressed in the direction parallel to those sides) is relatively constant for plates having a length to width ratio above 1.316. For the STP 3&4 spent fuel racks, the cell width (or cell inner dimension) is equal to 6.0". Therefore, the critical buckling load will not vary significantly for cell lengths greater than 1.316 x 6.0" = 7.896". For this reason, a cell length of 10" has been chosen for the FE model.

From the DYNARACK stress factor results, the maximum compressive stress on the outermost cell wall can be obtained as follows:

$$\sigma = 1.2 * Sy * R_6 \text{ (see Section 6.2.3.2)} = (1.2)(21{,}400 \text{ psi})(0.319) = 8{,}192 \text{ psi}$$

Therefore, in order to meet the stress criteria in Section 6.2.3, the cell walls must able to withstand a minimum compressive load of 8,192 psi × 3/2 = 12,228 psi. To that end, a uniformly distributed load of 170,000 lb (which exceeds 12,228 psi) is applied over the top edges of the cells in the finite element model. To initiate buckling, a 1 lb force is applied in lateral direction (perpendicularly outwards) to all the center line nodes of each cell wall.

The displaced shape of the 3 x 3 cell array under the maximum applied load is shown in Figure 6.7.2. The lateral displacement of node 292934 (which is the location of maximum displacement) is plotted in Figure 6.7.3 as a function of the applied load. The displacement plot is nearly linear, which indicates that there is no onset of buckling even at 1.5 times the actual load. Therefore, the cells remain in a stable configuration and the compressive stress limit from Section 6.2.3 is satisfied.

In addition, the following reference will be added to Section 6.12 of Holtec Report No. HI-2135462:

[6.7.9] Timoshenko, S.P and Gere, J., Theory of Elastic Stability, McGraw-Hill Book Company, Second Edition.

Finally, Figures 6.7.1, 6.7.2, and 6.7.3 will be revised as shown below.

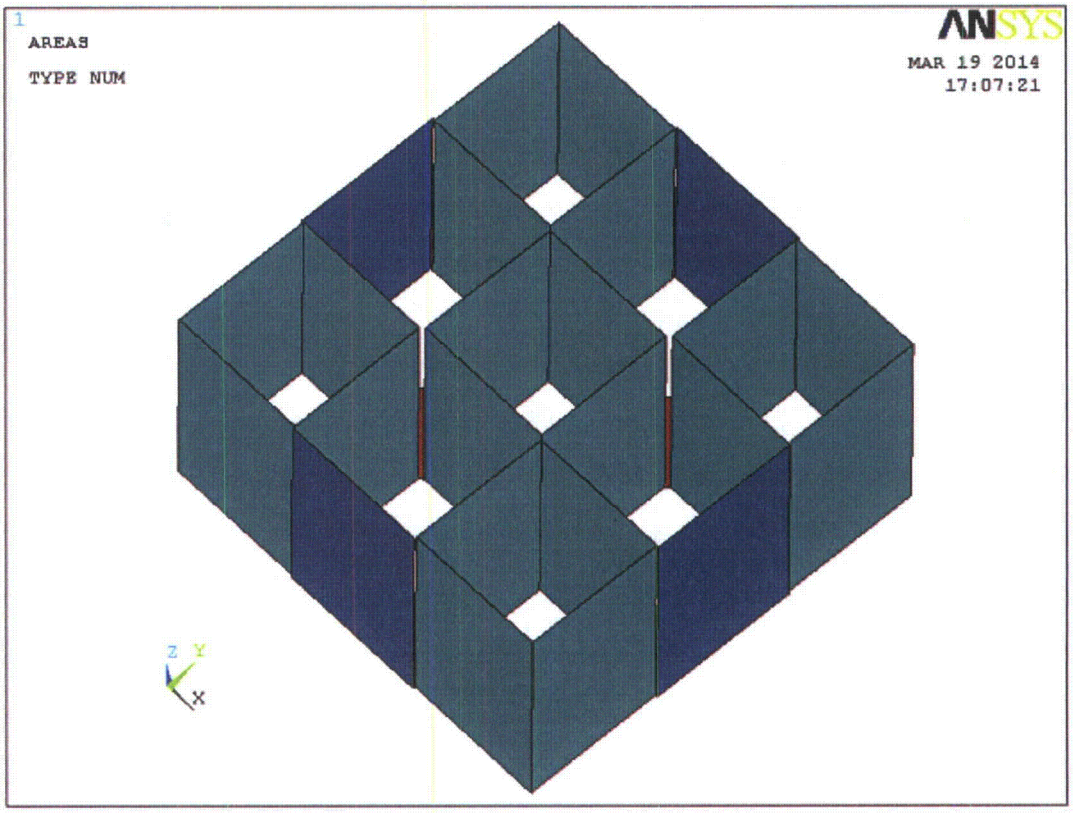

Figure 6.7.1 – Finite Element Model of 3 x 3 Cell Array

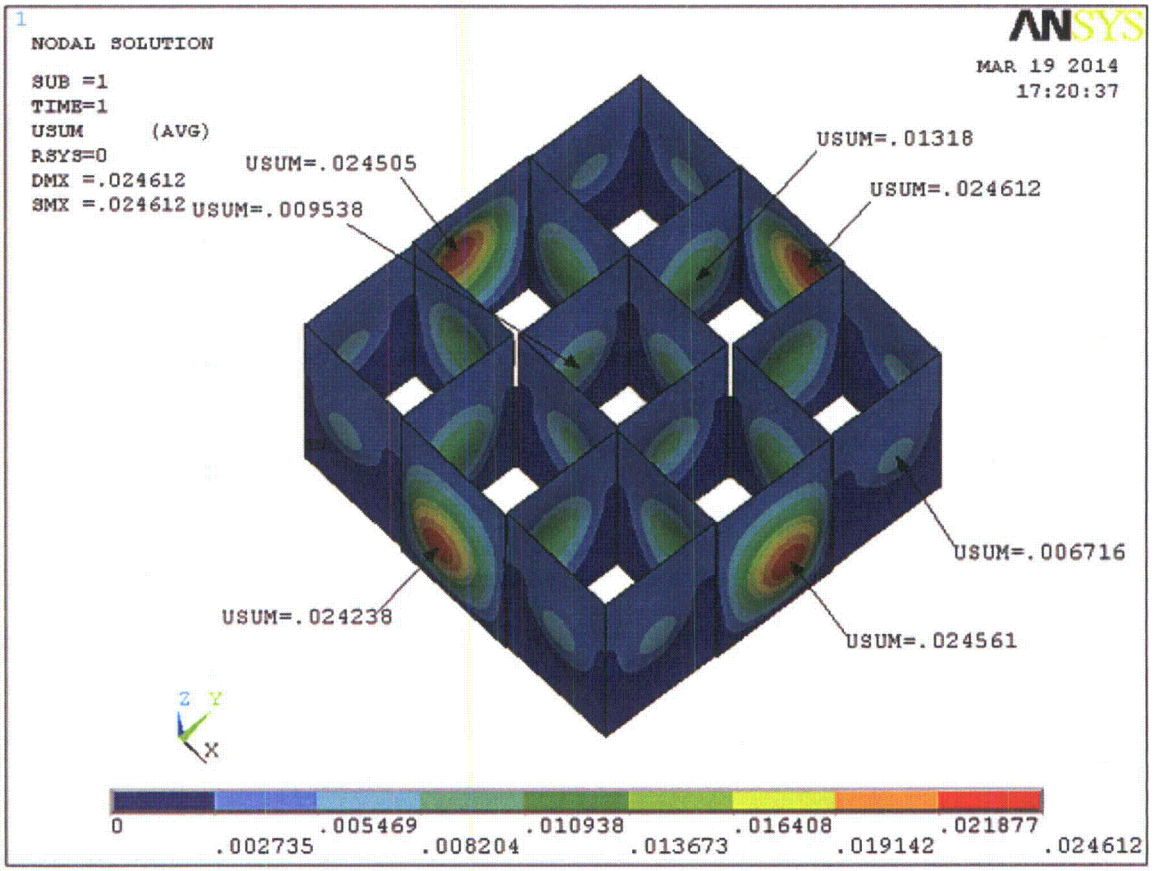

Figure 6.7.2 – Displaced Shape of 3 x 3 Cell Array Under Maximum Applied Load

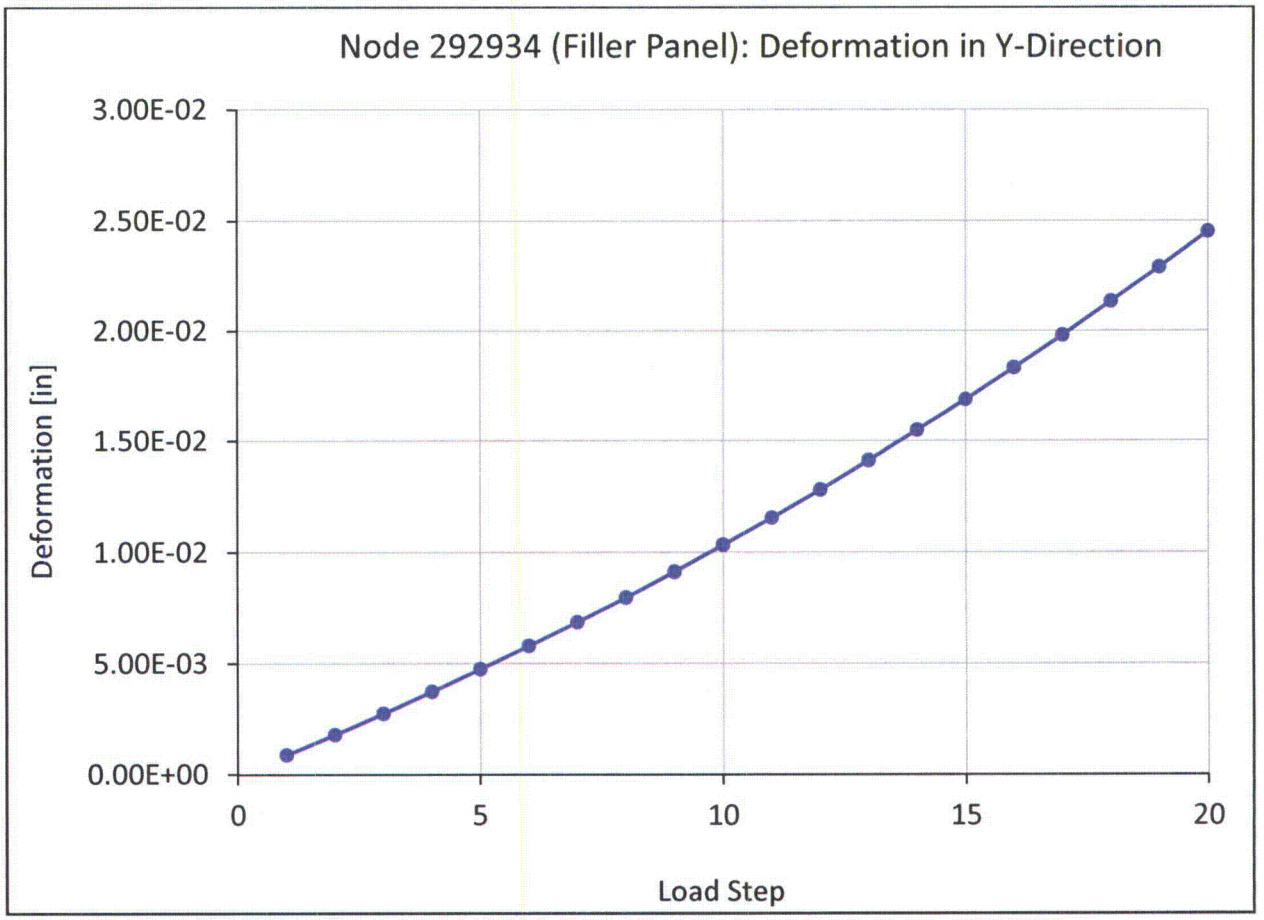

Figure 6.7.3 – Lateral Displacement vs. Applied Load for Node 292934

(2) The external sheathing is not credited as a load bearing member in any structural calculations. The area and moment of inertia of the sheathing are ignored when computing the gross section properties of the rack cell structure. That being said it is reasonable that the external sheathing significantly enhances the buckling capacity of the cell wall above a height of 4.875". Moreover, each sheathing panel has a total of 55" of weld length connecting it to the adjoining cell wall, which is more than the total length of weld between adjacent cells (36").

(3) The compressive load used in the buckling evaluation does indeed bound the maximum compressive stress at any location in any rack. Specifically, the applied load is derived from the maximum R_6 stress factor for combined flexure and compression (see Section 6.2.3.2 of HI-2135462) for the cell cross section of any rack from all of the dynamic simulations. Since the rack cell structure behaves like a cantilevered beam rooted at the base plate level, the maximum compressive stress in a cell wall occurs just above the base plate at a corner cell location. The figure below shows the rack and the cell wall that experiences the maximum compressive load. The magnitude of the compressive stress is 8,192 psi (as computed in NINA Letter, U7-C-NINA-NRC-130059, dated November 14, 2013, Attachment 5, Item 50).

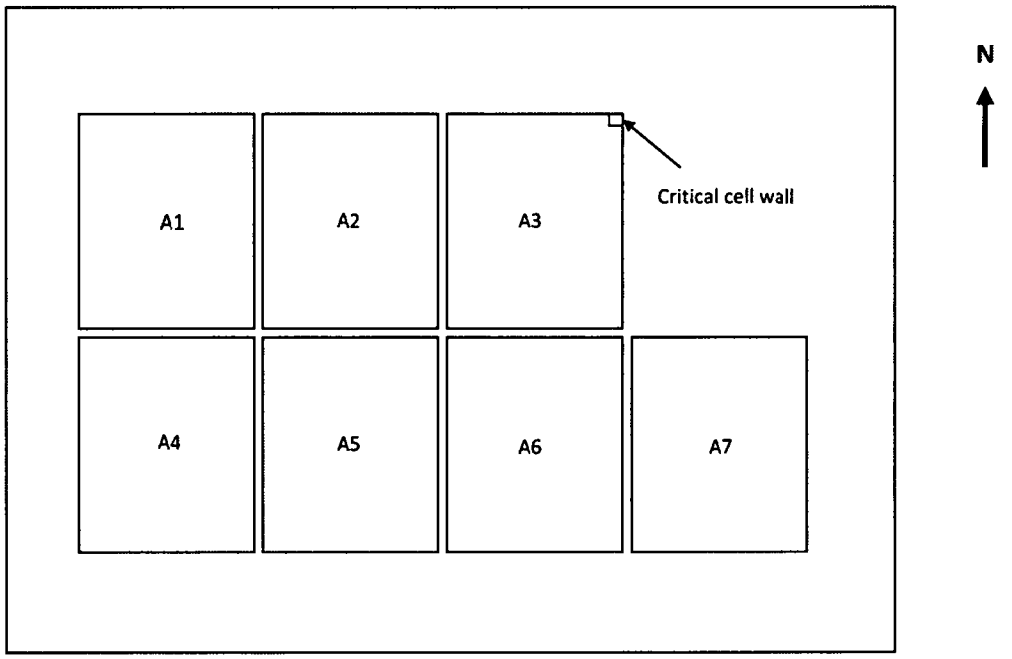
A1
A2
A3
A4
A5
A6
A7
Critical cell wall
N

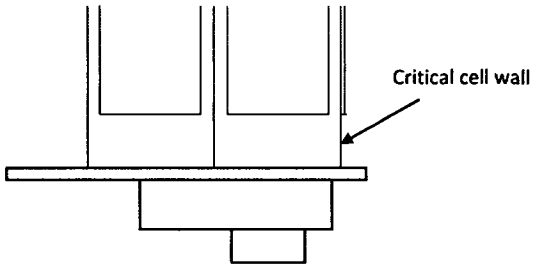
Critical cell wall

QUESTION:

NINA Letter, U7-C-NINA-NRC-130059, dated November 14, 2013, Attachment 5, Item 51 discusses punching shear analysis for the rack base plate at the pedestal location. The response states that seismic load on the pedestal is greater than fuel drop load. A punching shear calculation is added to Holtec Report No. HI-2135462 in Section 6.7.11. The equation uses 4 times the length of one side (13.5") of the female pedestal block in the calculation of the shear area. Considering that only 2 sides of the female pedestal are available at the corners, the staff requests that the applicant provide the technical basis for using 4 times the length of one side of the pedestal block in the calculation for the shear area.

RESPONSE:

NINA Letter, U7-C-NINA-NRC-130059, dated November 14, 2013, Attachment 5, Item 51, added a description of the punching shear calculation to Holtec Report HI-2135462, Section 6.7.11, Punching Shear Analysis of Rack Baseplate. The calculation described considers a four sided area, but it also credits only 50% of the base plate thickness. Therefore, the calculated shear capacity would remain unchanged if only 2 sides of the female pedestal and the full base plate thickness were credited.

HI-2135462, Section 6.7.11, Punching Shear Analysis of Rack Baseplate, previously submitted with Attachment 5, Item 51, will be revised as shown in the gray shaded text below to provide a better description of the calculation.

6.7.11 Punching Shear Analysis of Rack Baseplate

The only credible failure mode for the rack baseplate is a punching shear failure due to the concentrated load transmitted by a support pedestal under SSE conditions. Bending stresses in the baseplate are not significant since each storage cell is welded to the top surface of the baseplate creating a highly rigid structure. Therefore, only a punching shear analysis is performed for the rack baseplate.

The analysis demonstrates that the maximum vertical load on a single support pedestal (515,000 lb per Table 6.6.1) is less than the force necessary for the 13.5" square pedestal block to punch through the 1.5" thick baseplate, which is conservatively calculated as follows:

$$F_v = 2 \cdot L \cdot t \cdot (0.72 \cdot S_y)$$

where F_v is the punching shear capacity of the baseplate, L is the side length of the pedestal block (= 13.5"), t is the thickness of the baseplate (= 1.5"), and Sy is the minimum yield strength of the baseplate material (= 21,400 psi per Table 6.5.1). The above equation yields F_v = 624,024 lb, which exceeds the maximum pedestal load. Therefore, a punching shear failure of the rack baseplate will not occur.

The maximum impact load on the rack baseplate due to an accidental drop of a fuel assembly from a height of 1.8 meters above the top of rack is less than the maximum vertical load on a support pedestal due to SSE loading. Therefore, the above punching shear analysis is bounding for the fuel drop impact loads.

QUESTION:

NINA Letter, U7-C-NINA-NRC-130059, dated November 14, 2013, Attachment 5, Item 65 discusses how equipment storage areas around the pool will be controlled, evaluated, and documented, to ensure that the design-basis seismic analysis of racks and pool walls reflects actual as-built gap conditions. The response states that "to ensure there are no impacts between the racks and equipment stored around the perimeter of the spent fuel pool, there is an exclusion zone of 7 inches around the perimeter of the racks where equipment storage is prohibited." The staff determined that specifying an exclusion zone can avoid impact between the racks and the equipment, provided it is conservatively defined with a suitable margin on the maximum predicted displacement at the top of the racks (6.78"). The staff notes that a 7" exclusion zone leaves very little margin, and requests that the applicant provide its technical basis for specifying 7". In addition, the specification of an exclusion zone does not address the effect that fluid gap reductions may have on the rack structural response, as a result of changes in the fluid coupling loads. Therefore, the applicant is requested to provide the technical basis for concluding that fluid gap reductions due to adding equipment has insignificant effect on the rack structural response.

RESPONSE:

This response supersedes Item 65 of Attachment 5 to NINA Letter U7-C-NINA-NRC-130059 dated November 14, 2013. The exclusion zone was originally set at 7" in order to preclude impacts between the spent fuel racks and any equipment stored around the perimeter of the spent fuel pool. The 7" dimension was chosen based on the maximum rack displacements in Table 6.6.2 of Holtec Report No. 2135462 (see below). In the original determination of the exclusion zone, however, the potential sliding of the bearing pads was not considered. The bearing pads situated along the perimeter of the spent fuel rack array project beyond the envelope of the rack bumper bars by 5.41". Therefore, if the bearing pads slide along the SFP floor (instead of the rack pedestals sliding atop the bearing pads) by 4.72", which equals the maximum rack displacement at its base (see Table 6.6.2), then the bearing pads could reach as far as 10.13 inches beyond the initial envelope of the bumper bars. In order to prevent the bearing pads from encroaching into the equipment storage area, the exclusion zone has been increased to 11".

In order to substantiate the effectiveness of the exclusion zone, two additional Whole Pool Multi-Rack (WPMR) simulations have been performed in which the rack-to-wall gaps have been conservatively reduced to 7 inches around the entire perimeter of the spent fuel rack. The rack-to-wall gap of 7 inches represents the distance from the outside face of the bumper bar located near the top of the rack to the nearest structure (i.e., equipment stored around the perimeter of the spent fuel pool). Additionally, the fluid gaps around the perimeter of the racks have all been reduced to 7.5 inches. The fluid gaps are 0.5 inches greater than the rack-to-wall gaps (i.e., impact gaps) due to the thickness of the bumper bars at the top of the rack (i.e., bumper bars extend 0.5 inches beyond the cell wall perimeter).

Apart from the reduction in the rack-to-wall gaps, the first simulation is identical to run number 18 (which produced the maximum top of rack displacement) from Section 6.6 of Holtec Report No. HI-2135462. The second simulation also considers reduced rack-to-wall gaps of 7 inches and is otherwise identical to run number 19 (which produced the maximum stress factor) from Section 6.6 of Holtec Report No. HI-2135462. These new runs will be identified in Holtec Report No. HI-2135462 as run numbers 25 and 26, respectively.

The results for the major parameters of interest for run numbers 18, 19, 25 and 26 are tabulated below for comparison.

Result	**Calculated Value**			
	Run 18	**Run 19**	**Run 25**	**Run 26**
Maximum Top of Rack Displacement, in	6.78	2.99	1.724	2.99
Maximum Base Plate Displacement, in	1.05	1.00	0.358	0.356
Maximum Stress Factor	0.504	0.546	0.317	0.348
Maximum Fuel-to-Cell Impact Load, lbf	1,548	1,774	1,512	1,718
Maximum Vertical Load on a Single Pedestal, lbf	423,000	515,000	249,000	308,000
Maximum Shear Load on a Single Pedestal, lbf	317,000	282,000	193,000	174,000

The above table shows that all of the results for the major parameters of interest decrease (in many cases significantly) when the rack-to-wall gaps are reduced to 7 inches. This is expected since the reduced rack-to-wall gaps lead to an increase in the fluid coupling resistance, which in turn suppresses the seismic response of the spent fuel racks. Although run numbers 25 and 26 have been performed based on a 7 inch exclusion zone, it is evident from the results that a decrease in the perimeter gap causes a decrease in the rack displacements. Thus, the 11 inch exclusion zone, which has been established based on the displacement results corresponding to the maximum rack-to-wall gaps, is more than sufficient to preclude impacts between stored equipment and the spent fuel racks, including the bearing pads.

Section 6.6, Dynamic Simulations, of Holtec Report No. HI-2135462 will be revised as shown in gray shaded text below to include run numbers 25 and 26 (as well as run numbers 22 through 24 and 27 through 29, which are discussed in other RAI responses). In addition, Tables 6.6.1.a, 6.6.1.b, and 6.6.2 of Holtec Report No. HI-2135462 have been updated to reflect all 29 dynamic simulations.

6.6 Dynamic Simulations

As shown in Figure 1.1.1, the layout will contain seven (7) ABWR racks. Five sets of time histories were generated using EZ-FRISK as described in Section 6.5.2. Run numbers 1 through 5 are associated with the coefficient of friction (COF) value 0.2. Run numbers 6 through 10 are associated with the COF value 0.5, and finally, run numbers 11 through 15 are associated with the COF value 0.8 (see table below).

Run numbers 16 through 21 and run number 27 are sensitivity runs, which are all variants of run number 11. Run number 11 was chosen as the basis for the sensitivity analysis for the following reasons:

1) Run 11 produced the maximum top of rack displacement among the 15 base runs.
2) Run 11 produced the 3rd highest maximum vertical load on a single pedestal among the 15 base runs (which was within 3.9% of the overall maximum value)
3) Run 11 produced the 2nd highest fuel-to-cell impact load among the 15 base runs (which was within 5.3% of the overall maximum value)
4) Run 11 produced the 4th highest stress factor from among the 15 base runs (which was within 15.6% of the overall maximum value)

Based on the above, run number 11 was judged to be the most severe loading condition for the racks. Thus, the sensitivity runs were all performed using a COF of 0.8 and Time History Set 1 (shown in the Table 6.6.1.a).

- Run number 16 considers increased gaps to reflect the maximum tolerance values (+1/2" between racks). The gaps are modified in order to demonstrate the variation in results due to installation tolerances.
- Run number 17 considers a partially loaded rack configuration. The loaded racks are shown in Figure 6.6.1. This configuration was chosen because it considers the full range of fuel loading conditions (i.e., from a completely empty rack to a fully loaded rack).
- Run numbers 18 and 19 are identical to the bounding run (Run #11), except that the impact spring rates, as well as the rack beam stiffnesses, are uniformly decreased and increased by 20%, respectively. The purpose of run numbers 18 and 19 is to measure the sensitivity of the dynamic results to variations in the stiffness properties.
- Run numbers 20 and 27 are identical to the bounding run (Run #11), except that the integration time step is reduced by factors of 2 and 4, respectively, in order to verify that the solution is converged.
- Run number 21 simulates the start of plant operation - all racks are empty and submerged in water.

Run numbers 22 through 24 are sensitivity runs, which confirm that the maximum rack sliding displacements will be within the limits of the bearing pads. Run number 22 is identical to run number 17 except that the COF for all pedestals is reduced to 0.2.

Run number 23 is identical to run number 2 except that the integration time step is reduced to 5×10^{-6} sec. Run number 24 is identical to run number 2 except that the racks are partially loaded as shown in Figure 6.6.1.

In order to substantiate the establishment of the rack exclusion zone, two additional runs have been performed in which the rack-to-wall gaps have been conservatively reduced to 7" around the entire perimeter of the spent fuel rack layout. The rack-to-wall gap of 7 inches represents the distance from the outside face of the bumper bar located near the top of the rack to the nearest structure (i.e., equipment stored around the perimeter of the spent fuel pool). Additionally, the fluid gaps around the perimeter of the racks have all been reduced to 7.5 inches. The fluid gaps are 0.5 inches greater than the rack-to-wall gaps (i.e., impact gaps) due to the thickness of the bumper bars at the top of the rack (i.e., bumper bars extend 0.5 inches beyond the cell wall perimeter). Apart from the reduction in the rack-to-wall gaps, the first simulation is identical to run number 18 (which produced the maximum top of rack displacement). The second simulation also considers reduced rack-to-wall gaps of 7 inches and is otherwise identical to run number 19 (which produced the maximum stress factor). These two runs are identified as run numbers 25 and 26. It is noted that the actual size of the exclusion zone is 11 inches, which is greater than the analyzed dimension (i.e., 7 inches). The use of a smaller gap dimension for run numbers 25 and 26 is conservative provided that the displacement results do not indicate any impacts with the boundary wall.

Finally, run numbers 28 and 29 are identical to run number 15 (which produced the maximum rack-to-rack impact load at bumper bar elevation) except that the top-of-rack impact spring rate is increased by approximately 20% and 50%, respectively.

All simulations consider SSE excitation. The results of the simulations are compared to the stress and kinematic criteria in section 6.2. All 29 runs are summarized in Table 6.6.1.a.

Table 6.6.1.a
Simulation Listing

Coefficient of Friction	Run Number	Loading Configuration	Seismic Input	Integration Time Step (sec)	% of Calculated Rack Beam Stiffness and Impact Spring Rates
0.2	1	Fully Loaded	Set 1	1×10^{-5}	100%
	2	Fully Loaded	Set 2	1×10^{-5}	100%
	3	Fully Loaded	Set 3	1×10^{-5}	100%
	4	Fully Loaded	Set 4	1×10^{-5}	100%
	5	Fully Loaded	Set 5	1×10^{-5}	100%
0.5	6	Fully Loaded	Set 1	1×10^{-5}	100%
	7	Fully Loaded	Set 2	1×10^{-5}	100%
	8	Fully Loaded	Set 3	1×10^{-5}	100%
	9	Fully Loaded	Set 4	1×10^{-5}	100%
	10	Fully Loaded	Set 5	1×10^{-5}	100%
0.8	11	Fully Loaded	Set 1	1×10^{-5}	100%
	12	Fully Loaded	Set 2	1×10^{-5}	100%
	13	Fully Loaded	Set 3	1×10^{-5}	100%
	14	Fully Loaded	Set 4	1×10^{-5}	100%
	15	Fully Loaded	Set 5	1×10^{-5}	100%
Bounding Case (0.8)	16	Fully Loaded, modified gaps (max. tolerance)	Bounding Case (Set 1)	1×10^{-5}	100%
Bounding Case (0.8)	17	Mixed Loading	Bounding Case (Set 1)	1×10^{-5}	100%
Bounding Case (0.8)	18	Fully Loaded	Bounding Case (Set 1)	1×10^{-5}	80%
Bounding Case (0.8)	19	Fully Loaded	Bounding Case (Set 1)	1×10^{-5}	120%
Bounding Case (0.8)	20	Fully Loaded	Bounding Case (Set 1)	5×10^{-6}	100%
Bounding Case (0.8)	21	Empty	Bounding Case (Set 1)	1×10^{-5}	100%
0.2	22	Mixed Loading	Bounding Case (Set 1)	1×10^{-5}	100%

Table 6.6.1.a
Simulation Listing

Coefficient of Friction	Run Number	Loading Configuration	Seismic Input	Integration Time Step (sec)	% of Calculated Rack Beam Stiffness and Impact Spring Rates
0.2	23	Fully Loaded	Set 2	5×10^{-6}	100%
0.2	24	Mixed Loading	Set 2	1×10^{-5}	100%
Bounding Case (0.8)	25	Fully Loaded, modified gaps (7" exclusion zone)	Bounding Case (Set 1)	1×10^{-5}	80%
Bounding Case (0.8)	26	Fully Loaded, modified gaps (7" exclusion zone)	Bounding Case (Set 1)	1×10^{-5}	120%
Bounding Case (0.8)	27	Fully Loaded	Bounding Case (Set 1)	2.5×10^{-6}	100%
0.8	28	Fully Loaded	Set 5	1×10^{-5}	100% (except rack-to-rack impact spring at top of rack increased by 20%)
0.8	29	Fully Loaded	Set 5	1×10^{-5}	100% (except rack-to-rack impact spring at top of rack increased by 50%)

Table 6.6.1.b (continued)
Maximum Values of Stress Factors and Impact Loads

COF	Run No.	Max. Stress Factor (defined in Section 6.2)	Max. Vertical Load on Single Pedestal (lbf)	Max. Shear Load on Single Pedestal (lbf) (X or Y)	Max Fuel to Cell Wall Impact (lbf)	Max. Rack-to-Rack Impacts (lbf)	
						Top	Baseplate
0.2	1	0.158	224,000	43,500	1,392	-	-
	2	0.160	219,000	41,100	1,295	-	-
	3	0.181	260,000	49,100	1,309	-	226,420
	4	0.186	268,000	51,400	1,265	-	-
	5	0.183	268,000	52,200	1,212	-	83,050
0.5	6	0.385	492,000	199,000	1,527	-	-
	7	0.365	370,000	156,000	1,489	-	-
	8	0.374	389,000	192,000	1,468	-	56,690
	9	0.325	359,000	177,000	1,545	-	-
	10	0.401	470,000	202,000	1,345	-	-
0.8	11	0.450	487,000	252,000	1,612	-	-
	12	0.507	389,000	256,000	1,524	-	-
	13	0.533	443,000	269,000	1,424	-	-
	14	0.388	361,000	268,000	1,703	-	-
	15	0.508	507,000	321,000	1,380	188,780	-
Sensitivity Runs							
0.8	16	0.424	509,000	241,000	1,683	-	-
	17	0.485	413,000	248,000	1,695	-	71,520
	18	0.504	423,000	317,000	1,548	-	-
	19	0.546	515,000	282,000	1,774	-	-
	20	0.483	458,000	276,000	1,692	-	-
	21	0.097	72,800	42,700	-	-	-
0.2	22	0.161	231,000	41,000	1,250	-	139,220
	23	0.164	223,000	41,000	1,188	-	-
	24	0.155	208,000	40,000	876	-	99,930
0.8	25	0.317	249,000	193,000	1,512	-	-
	26	0.348	308,000	174,000	1,718	-	-

COF	Run No.	Max. Stress Factor (defined in Section 6.2)	Max. Vertical Load on Single Pedestal (lbf)	Max. Shear Load on Single Pedestal (lbf) (X or Y)	Max Fuel to Cell Wall Impact (lbf)	Max. Rack-to-Rack Impacts (lbf)	
						Top	Baseplate
0.8	27	0.477	436,000	275,000	1,697	-	-
	28	0.442	507,000	250,000	1,347	200,540	-
	29	0.442	507,000	250,000	1,347	210,480	-

Table 6.6.2 Rack Displacements		
Run Number	Maximum Rack displacement relative to floor (inch)	
	Top of Rack	Baseplate
1	2.64	2.62
2	4.81	4.70
3	4.80	4.64
4	4.37	4.31
5	3.63	3.38
6	3.47	0.99
7	3.46	1.66
8	2.63	1.53
9	3.53	1.31
10	5.12	1.43
11	5.46	1.02
12	3.49	1.32
13	3.01	0.58
14	2.48	0.62
15	4.70	0.64
16	2.82	0.86
17	3.58	1.35
18	6.78	1.05
19	2.99	1.00
20	4.90	1.05
21	1.49	0.86
22	3.03	2.97
23	4.84	4.72
24	3.75	3.66
25	1.72	0.36

Table 6.6.2 (continued) Rack Displacements		
Run Number	Maximum Rack displacement relative to floor (inch)	
	Top of Rack	Baseplate
26	2.99	0.35
27	5.02	0.95
28	4.70	0.64
29	4.70	0.64

09.01.02-67

QUESTION:

Holtec Report HI-2135462, Section 3.5, "In-Service Surveillance of Neutron Absorber," contains table 3.5.1 which describes the recommended coupon withdrawal schedule for the Metamic surveillance program. In this table after coupon #8 is withdrawn, the applicant recommends that the next coupon be withdrawn for testing 12 years later. Metamic has been previously approved by the Commission for use on operating reactors' spent fuel pool. However, the staff has not approved a surveillance program with more than 10 years between coupon testing. Therefore, the staff requests that the applicant provide an explanation on the reasoning behind their recommended coupon measurement schedule.

RESPONSE:

Holtec Report HI-2135462, Section 3.5.2, Coupon Surveillance Program, specifies, "the coupon surveillance program uses a tree with twelve (12) test coupons" which are manufactured from the same lots of Metamic that are used in the spent fuel rack. Consistent with good engineering practice, HI-2135462 Table 3.5.1, Recommended Coupon Measurement Schedule, specifies frequent testing during the early life of the spent fuel rack and less frequent testing after performance of the installed lot of Metamic has been demonstrated. Specifically, HI-2135462 Table 3.5.1 establishes a minimum surveillance interval of every 2 years during the first 10 years after the racks are submerged under water with a maximum interval of every 12 years beginning after year 36. The coupon surveillance schedule in HI-2135462 Table 3.5.1 requires the use of ten (10) of the twelve (12) installed Metamic test coupons.

HI-2135462 Table 3.5.1 will be revised, as shown in the gray highlighted changes shown below, to specify that no surveillance interval will exceed 10 years during the 60-year life of the plant.

TABLE 3.5.1 RECOMMENDED COUPON MEASUREMENT SCHEDULE	
Coupon	Years[1]
1	2
2	4
3	6
4	8
5	12
6	18
7	26
8	36
9	~~48~~ 46
10	~~60~~ 56

1 The years pertain to those after the installation of the SFP storage racks (i.e. racks are submerged under water).

Limiting the maximum surveillance interval to 10 years (versus 12 years) during the 60 year life of the spent fuel racks does not require the use of any additional Metamic test coupons. Two (2) test coupons will remain available for contingencies that warrant additional coupon testing during or after the 60 year life of the plant. Additionally, an in-situ measurement program, such as those described in NEI 12-16, Guidance for Performing Criticality Analyses of Fuel Storage at Light-Water Reactor Power Plants, can be utilized in the very unlikely event that all Metamic test coupons are exhausted and the spent fuel racks remain in service.

09.01.02-68

QUESTION:

Holtec Report No. HI-2135462, Section 3.4, "Compatibility with Environment," mentions that the spent fuel pool environment will not corrode the neutron absorbing material, Metamic, and for that reason will not release aluminum debris to the pool. However, the spent fuel pool needs to be monitored for aluminum and other chemical substances that could be damaging to the fuel. Therefore, the staff requests that the applicant provide additional information on the monitoring of the spent fuel pool water.

RESPONSE:

Holtec Report HI-2135462, Section 3.4, Compatibility with Environment, provides the basis for the conclusion that "as the SFP water does not corrode the Metamic, it can be concluded that corrosion will not reduce the design life of the Metamic." Additionally, the Metamic coupon testing program described in Section 3.5.2 and discussed in the response to RAI 09.01.02-67 will provide a high degree of assurance throughout the life of the racks that significant corrosion of Metamic that would interfere with its design function is identified in a timely manner. Therefore, routine monitoring of spent fuel pool water for aluminum is not currently anticipated.

STP will follow the EPRI BWR Water Chemistry Guidelines described in DCD reference 5.2-3. The EPRI BWR Water Chemistry Guidelines do not require testing of reactor water for aluminum.

In the event that the Metamic coupon surveillance program or industry experience indicates unexpected degradation of the Metamic material, testing for aluminum would be considered in addition to the requirements of the EPRI BWR Water Chemistry Guidelines if such testing is indicated by industry experience.

Affidavit

Holtec Center, One Holtec Drive, Marlton, NJ 08053
Telephone (856) 797-0900
Fax (856) 797-0909

Holtec International Document ID AFFI-2294-04

AFFIDAVIT PURSUANT TO 10 CFR 2.390

I, Debabrata Mitra-Majumdar, being duly sworn, depose and state as follows:

(1) I have reviewed the information described in paragraph (2) which is sought to be withheld, and am authorized to apply for its withholding.

(2) The information sought to be withheld is information provided within attachments to the responses for RAIs 09.01.02-38 and 09.01.02-48, which contains Holtec Proprietary information and is appropriately marked as such.

(3) In making this application for withholding of proprietary information of which it is the owner, Holtec International relies upon the exemption from disclosure set forth in the Freedom of Information Act ("FOIA"), 5 USC Sec. 552(b)(4) and the Trade Secrets Act, 18 USC Sec. 1905, and NRC regulations 10CFR Part 9.17(a)(4), 2.390(a)(4), and 2.390(b)(1) for "trade secrets and commercial or financial information obtained from a person and privileged or confidential" (Exemption 4). The material for which exemption from disclosure is here sought is all "confidential commercial information", and some portions also qualify under the narrower definition of "trade secret", within the meanings assigned to those terms for purposes of FOIA Exemption 4 in, respectively, Critical Mass Energy Project v. Nuclear Regulatory Commission, 975F2d871 (DC Cir. 1992), and Public Citizen Health Research Group v. FDA, 704F2d1280 (DC Cir. 1983).

AFFIDAVIT PURSUANT TO 10 CFR 2.390

(4) Some examples of categories of information which fit into the definition of proprietary information are:

a. Information that discloses a process, method, or apparatus, including supporting data and analyses, where prevention of its use by Holtec's competitors without license from Holtec International constitutes a competitive economic advantage over other companies;

b. Information which, if used by a competitor, would reduce his expenditure of resources or improve his competitive position in the design, manufacture, shipment, installation, assurance of quality, or licensing of a similar product.

c. Information which reveals cost or price information, production, capacities, budget levels, or commercial strategies of Holtec International, its customers, or its suppliers;

d. Information which reveals aspects of past, present, or future Holtec International customer-funded development plans and programs of potential commercial value to Holtec International;

e. Information which discloses patentable subject matter for which it may be desirable to obtain patent protection.

The information sought to be withheld is considered to be proprietary for the reasons set forth in paragraph 4.b, above.

(5) The information sought to be withheld is being submitted to the NRC in confidence. The information (including that compiled from many sources) is of a sort customarily held in confidence by Holtec International, and is in fact so held. The information sought to be withheld has, to the best of my knowledge and belief, consistently been held in confidence by Holtec International. No public disclosure has been made, and it is not available in public sources. All disclosures to third parties, including any required transmittals to the NRC, have been made, or must be made, pursuant to regulatory provisions or proprietary

agreements which provide for maintenance of the information in confidence. Its initial designation as proprietary information, and the subsequent steps taken to prevent its unauthorized disclosure, are as set forth in paragraphs (6) and (7) following.

(6) Initial approval of proprietary treatment of a document is made by the manager of the originating component, the person most likely to be acquainted with the value and sensitivity of the information in relation to industry knowledge. Access to such documents within Holtec International is limited on a "need to know" basis.

(7) The procedure for approval of external release of such a document typically requires review by the staff manager, project manager, principal scientist or other equivalent authority, by the manager of the cognizant marketing function (or his designee), and by the Legal Operation, for technical content, competitive effect, and determination of the accuracy of the proprietary designation. Disclosures outside Holtec International are limited to regulatory bodies, customers, and potential customers, and their agents, suppliers, and licensees, and others with a legitimate need for the information, and then only in accordance with appropriate regulatory provisions or proprietary agreements.

(8) The information classified as proprietary was developed and compiled by Holtec International at a significant cost to Holtec International. This information is classified as proprietary because it contains detailed descriptions of analytical approaches and methodologies not available elsewhere. This information would provide other parties, including competitors, with information from Holtec International's technical database and the results of evaluations performed by Holtec International. A substantial effort has been expended by Holtec International to develop this information. Release of this information would improve a competitor's position because it would enable Holtec's competitor to copy our technology and offer it for sale in competition with our company, causing us financial injury.

AFFIDAVIT PURSUANT TO 10 CFR 2.390

(9) Public disclosure of the information sought to be withheld is likely to cause substantial harm to Holtec International's competitive position and foreclose or reduce the availability of profit-making opportunities. The information is part of Holtec International's comprehensive spent fuel storage technology base, and its commercial value extends beyond the original development cost. The value of the technology base goes beyond the extensive physical database and analytical methodology, and includes development of the expertise to determine and apply the appropriate evaluation process.

The research, development, engineering, and analytical costs comprise a substantial investment of time and money by Holtec International.

The precise value of the expertise to devise an evaluation process and apply the correct analytical methodology is difficult to quantify, but it clearly is substantial.

Holtec International's competitive advantage will be lost if its competitors are able to use the results of the Holtec International experience to normalize or verify their own process or if they are able to claim an equivalent understanding by demonstrating that they can arrive at the same or similar conclusions.

The value of this information to Holtec International would be lost if the information were disclosed to the public. Making such information available to competitors without their having been required to undertake a similar expenditure of resources would unfairly provide competitors with a windfall, and deprive Holtec International of the opportunity to exercise its competitive advantage to seek an adequate return on its large investment in developing these very valuable analytical tools.

Affidavit

Holtec International Document ID AFFI-2294-04

AFFIDAVIT PURSUANT TO 10 CFR 2.390

STATE OF NEW JERSEY)
) ss:
COUNTY OF BURLINGTON)

Dr. Debabrata Mitra-Majumdar, being duly sworn, deposes and says:

That he has read the foregoing affidavit and the matters stated therein are true and correct to the best of his knowledge, information, and belief.

Executed at Marlton, New Jersey, this 7th day of July, 2014.

Debabrata Mitra-Majumdar
Holtec International

Subscribed and sworn before me this 7th day of July, 2014.

MARIA C. MASSI
NOTARY PUBLIC OF NEW JERSEY
My Commission Expires April 25, 2015